ACTIVATION OF ERK/MAPK SIGNALING BY *Burkholderia pseudomallei* CYCLE INHIBITING FACTOR

NG Mei Ying
(B.Sc. (Hons.), NUS)

A THESIS SUBMITTED

FOR THE DEGREE OF MASTER OF SCIENCE

DEPARTMENT OF BIOCHEMISTRY

NATIONAL UNIVERSITY OF SINGAPORE

2016

DECLARATION

I hereby declare that the thesis is my original work and it has been written by me in its entirety. I have duly acknowledged all the sources of information which have been used in the thesis.
This thesis has also not been submitted for any degree in any university previously.

Hnang.

NG Mei Ying
31 July 2016

ACKNOWLEDGEMENTS

First of all, I would like to acknowledge the support of my supervisors. I am most grateful to Thilo for the past five years of mentorship. He has given me valuable guidance and constructive advice in my project throughout the years and allowed me to develop in my critical thinking and analytical skills. Apart from my Honours and M.Sc. projects, he has also given me the opportunity to explore various research topics I was curious and interested in.

I am also thankful to Yunn for her co-supervision and for supporting me as a Research Assistant in her lab as I complete my M.Sc. project. She has given me constant encouragement and her passion for research has been a motivation for me throughout the years.

I would like to acknowledge the efforts of our collaborators, Assistant Professor Mei-Wang Casey and Professor Patrick Casey for their inputs, without which the project would have been incomplete.

I am also hugely indebted to Dr Tan Hwee Tong, Professor Maxey Chung and the NUS Protein and Proteomics Centre for their sustained efforts in the mass spectrometry work on SOS1.

We are grateful to Millenium Pharmaceuticals, Inc. for providing us with the Nedd8 E1 activating enzyme inhibitor MLN4924 and Addgene for the plasmid constructs.

Finally, I am very grateful to be part of two brilliant labs, the TH Lab and the GYH Lab.

TABLE OF CONTENTS

SUMMARY

Cycle inhibiting factors (Cifs) are virulence proteins secreted by the type III secretion system of some Gram-negative pathogenic bacteria including *Burkholderia pseudomallei.* Cif is known to function to deamidate Nedd8, leading to inhibition of Cullin E3 ubiquitin ligases (CRL) and consequently induction of cell cycle arrest. Here I show that Cif can function as a potent activator of MAPK/ERK signaling without significant activation of other signaling pathways downstream of receptor tyrosine kinases. Importantly, I found that the ability of Cif to activate ERK is dependent on its deamidase activity, but independent of Cullin E3 ligase inhibition. This suggests that apart from Nedd8, other cellular targets of Cif-dependent deamidation exist. I provide evidence that the mechanism involved in Cif-mediated ERK activation is dependent on recruitment of the Grb2-SOS1 complex to the plasma membrane. Further investigation revealed that Cif modifies the phosphorylation status of SOS1 in a region containing the CDC25-H and proline-rich domains. It is known that prolonged Cullin E3 ligase inhibition leads to cellular apoptosis. Therefore, I hypothesise that ERK activation is an important mechanism to counter the pro-apoptotic effects of Cif. Indeed, I show that Cif-dependent ERK activation promotes phosphorylation of the pro-apoptotic protein Bim, thereby conferring a pro-survival signal. In summary, I identified a novel deamidation-dependent mechanism of action of the *B. pseudomallei* virulence factor Cif/CHBP to activate MAPK/ERK signaling. ERK activation may counter the pro-apoptotic effects of Cif and hence promote bacterial pathogenicity. My study also

demonstrates that bacterial proteins such as Cif can serve as useful molecular tools to uncover novel aspects of mammalian signaling pathways.

LIST OF TABLES

LIST OF FIGURES

LIST OF SYMBOLS

Cif	cycle inhibiting factor
CIP	calf intestinal alkaline phosphatase
CRL	cullin RING E3 ubiquitin ligase
DH	Dbl homology
DMSO	dimethyl sulfoxide
Dn	dominant negative
EDTA	ethylenediaminetetraacetic acid
EGTA	ethylene glycol-bis(2-aminoethylether)-*N,N,N′,N′*-tetraacetic acid
ERK	extracellular signal-regulated kinase
FRAT1	frequently rearranged in advanced T-cell lymphomas **1**
GDP	guanosine diphosphate
GEF	guanine nucleotide exchange factor
GTP	guanosine triphosphate
GFP	green fluorescent protein
GSK3β	Glycogen synthase kinase 3 beta
Grb2	growth factor receptor-bound protein 2

HEK293T	human embryonic kidney 293 cells stably expressing SV40 large T antigen
HIF-1α	hypoxia-inducible factor 1-alpha
IκBα	inhibitor of κappaB kinase alpha
IP	immunoprecipitation
JNK	Jun amino-terminal kinase
LC-MS/MS	liquid chromatography–mass spectrometry
MAPK	mitogen-activated protein kinase
PAGE	polyacrylamide gel electrophoresis
PCR	polymerase chain reaction
PH	Pleckstrin homology
PI3K	phosphoinositide 3-kinase
REM	Ras exchanger motif
RTK	receptor tyrosine kinase
SAPK	stress-activated protein kinase
SDS	sodium dodecyl sulfate
SH2	src homology 2 domain
SH3	src homology 3 domain
SOS	son of sevenless
STAT3	signal transducer and activator of transcription 3

LIST OF PUBLICATIONS

1. Boh, B.K., Ng, M.Y., Leck, Y.C., Shaw, B., Long, J., Sun, G.W., Gan, Y.H., Searle, M.S., Layfield, R., Hagen, T. 2011. Inhibition of Cullin RING ligases by cycle inhibiting factor: evidence for interference with Nedd8-induced conformational control. *J. Mol. Biol*. **413**, 430-437.

2. Ng, M.Y., Wang, M., Casey, P.J., Gan, Y.H., Hagen, T. 2016. Activation of MAPK/ERK signaling by *Burkholderia pseudomallei* Cycle inhibiting factor (Cif). *PLoS One*. (submitted July 2016)

1. INTRODUCTION

1.1 *Burkholderia pseudomallei*: The causative agent of melioidosis

Burkholderia pseudomallei is a Gram-negative, environmental saprophyte that is commonly found in stagnant waters and muddy soils in endemic regions including many parts of Southeast Asia, Northern Australia, as well as other tropical regions (Currie *et al*., 2000; Leearasamee, 2000; White, 2003). Besides these primary ecological niches, *B. pseudomallei* is also capable of surviving within a wide range of hosts such as amoebae, nematodes, plants as well as many mammalian species including humans (Inglis *et al*., 2000; Gan *et al*., 2002; Holden *et al*., 2004; Lee *et al*., 2010; Sprague and Neubauer, 2004).

Infection with this opportunistic pathogen usually occurs via respiratory, percutaneous or oral routes, and causes a potentially life-threatening disease known as melioidosis (Dharakul and Songsivilai, 1999). Individuals with underlying predisposing risk factors associated with compromised immune responses, of which the most predominant is diabetes mellitus, are more susceptible to *B. pseudomallei* infection (White, 2003; Cheng and Currie, 2005; Wiersinga *et al*., 2006). Although the clinical manifestation and outcome of melioidosis vary widely, the most prevalent symptom is severe pulmonary distress, which can progressively lead to septicaemia and death (Asche, 1991; Suputtamongkol *et al*., 1994; Wiersinga *et al*., 2006). At present, the mortality rate resulting from *B. pseudomallei* infection remains exceptionally high because *B. pseudomallei* is intrinsically resistant to most existing

antibiotics and there is currently no licensed vaccine available (Dance, 1991; Chaowagul, 2000; Ngauy *et al*., 2005).

B. pseudomallei is a highly versatile intracellular bacterium that is adept at invading and surviving in different tissues and cell types (Jones *et al*., 1996; Galyov *et al*., 2010). It is well established that upon exposure, *B. pseudomallei* invades the mammalian host cells, escapes from the phagosomes, replicates within the host cytosol, and spreads from cell to cell by inducing cell fusion through multi-nucleated giant cell formation (Stevens *et al*., 2002; Burtnick *et al*., 2008). In order to mediate these processes, *B. pseudomallei* utilises a number of virulence mechanisms including the type III and type VI secretion systems (Stevens *et al*., 2004; Warawa and Woods, 2005; Cornelis, 2006; Jani and Cotter, 2010). These secretion systems are highly specialised machineries that allow the bacterium to dock on the host cell plasma membrane and translocate effector proteins across this surface membrane into the host cell cytosol or to directly inject effector proteins from within the host cytosol. The delivered effector proteins function to alter host cellular responses to establish an infection.

Of the hundreds of effector molecules of the type III secretion system identified to date, many have been reported to frequently target host cell nuclear factor κappaB (NF-κB) and mitogen-activated protein kinase (MAPK) signaling pathways (Mota and Cornelis, 2005). This is not surprising because both the NF-κB and MAPK signaling pathways function as host defense mechanisms against invading pathogens. As such, interference with these cellular signaling pathways allows the bacterium to suppress the host immune

response and support its replication and survival within the host cells.

1.2 Cycle Inhibiting Factor is a virulence effector of *B. pseudomallei*

Among the wide array of virulence effector proteins, Cycle inhibiting factors (Cifs) are one group of bacterial virulence proteins that are secreted by the type III secretion system of Gram-negative bacterial pathogens (Jubelin *et al*., 2009; Yao *et al*., 2009). Cif was initially discovered in enteropathogenic *Escherichia coli* (EPEC) and enterohemorrhagic *E. coli* (EHEC) and subsequently in four other pathogenic or symbiotic bacteria: *Burkholderia pseudomallei*, *Yersinia pseudotuberculosis*, *Photorhabdus luminescens* and *Photorhabdus asymbiotica* (De Rycke *et al*., 1997; Jubelin *et al*., 2009).

Upon injection into host cells, Cif is known to inhibit host cell cycle progression at both G_1/S and G_2/M phase transitions. This halt in cell cycle progression may play a role in promoting bacterial colonization of the host cells. It has been shown that the cell cycle arrest is induced as a result of stabilization of cyclin-dependent kinase inhibitors $p21^{waf1/cip1}$ and $p27^{kip1}$ (hereafter referred to as p21 and p27) (Samba-Louaka *et al*., 2008; Jubelin *et al*., 2010; Cui *et al*., 2010). Cellular concentrations of the cell cycle inhibitors p21 and p27 are normally tightly regulated via ubiquitination by cullin RING E3 ubiquitin ligases (CRLs). Ubiquitinated p21 and p27 are then targeted to the 26S proteasome for degradation (Tsvetkov *et al*., 1999; Carrano *et al*., 1999; Sutterlüty *et al*., 1999). Cif has been shown to inhibit CRL function, leading to the accumulation of p21 and p27 (Figure 1). Another mechanism through which Cif may interfere with the host cell bacterial defense is by inhibiting the

CRL-dependent IκB degradation (Figure 2). As a result, NF-κB activation upon bacterial infection is prevented (Cui *et al.*, 2010).

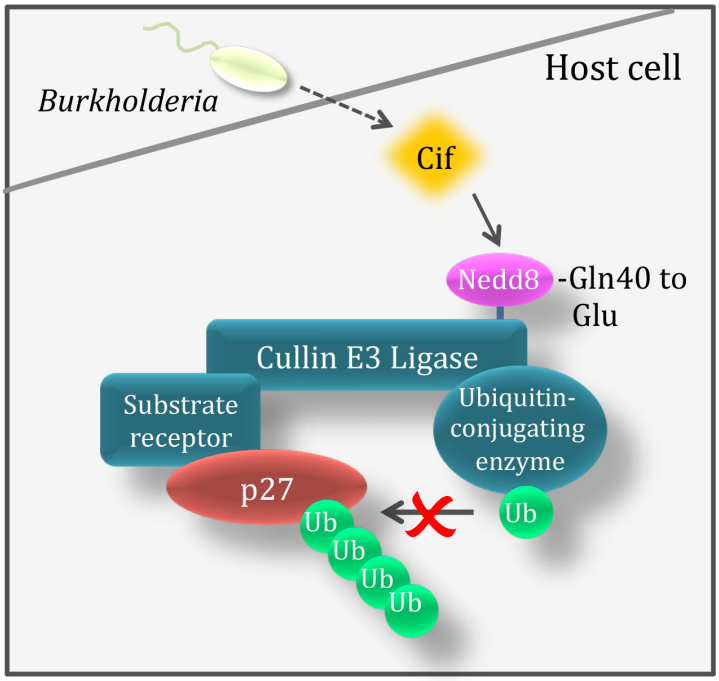

Figure 1. Cif inhibits Cullin E3 Ring ubiquitin ligase (CRL) function via deamidation of Nedd8, thereby leading to stabilisation of the CRL substrate p27.

CRLs constitute the largest family of E3 ubiquitin ligases, primarily due to their modular structure. There are six different Cullin homologous proteins, with each forming a scaffold onto which different E3 ligase complexes assemble (Petroski and Deshaies, 2005; Bosu and Kipreos; 2008). CRLs bind the RING subunit at the carboxy-terminus, which functions to recruit the ubiquitin-charged E2 ubiquitin-conjugating enzyme. At the amino-terminus, CRLs bind different substrate receptors, which are responsible for recruiting specific cellular substrate proteins. As a result of the assembly, the substrate is brought into close proximity to the ubiquitin-charged E2 enzyme, thus facilitating the transfer of ubiquitin from the E2 enzyme onto the substrate.

However, CRL-dependent ubiquitination of substrate proteins requires modification of CRL by the 76-amino acid ubiquitin-like protein Nedd8. Nedd8 conjugation to a conserved lysine residue in the carboxy-terminus of CRLs induces a conformational change in CRL that is required to activate its ubiquitination activity.

1.3 Cif functions as a deamidase

Recent studies have revealed that Cif functions as a deamidase that targets Nedd8 on Gln40, thus converting it into a glutamate (Cui *et al*., 2010) (Figure 1 and 2). Mechanistically, it has been shown that Nedd8 deamidation does not preclude the conjugation of Nedd8 onto the Cullin protein, but prevents the Nedd8 induced conformational change of the CRL complex (Boh *et al*., 2011; Yu *et al*., 2015). Consequently, the Cif-mediated enzymatic modification in Nedd8 results in a marked inhibition of CRL activity, thus preventing ubiquitination of substrate proteins by CRLs and leading to stabilization of p21, p27 and other CRL substrates. Hence, the cell cycle inhibitory effect of Cif is attributed to Cif-dependent inhibition of CRL activity involving Nedd8 deamidation.

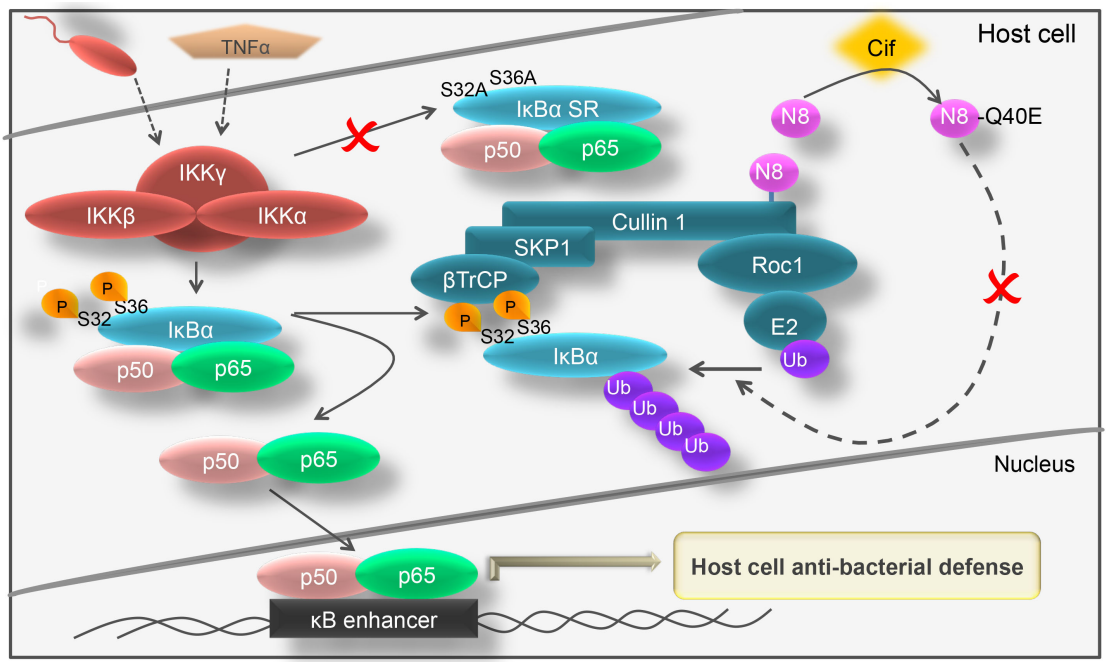

Figure 2. Cif deamidates Nedd8, thereby leading to inhibition of the NF-κB mediated host cell anti-bacterial defense.

1.4 Aim of this project

In my Honours project, I discovered that apart from CRL inhibition, Cif also exerts additional effects in host cells. Specifically, I found that Cif induces a potent and selective activation of the pro-survival ERK MAPK pathway. The goal of this project was hence to characterise the mechanism through which Cif activates ERK and address the potential significance and physiological role of Cif-mediated ERK activation in bacterial pathogenicity.

2. MATERIALS AND METHODS

Cell culture and transfection

HEK293T cells were cultured in Dulbecco's modified eagle medium (DMEM) (Invitrogen) supplemented with 10% (vol/vol) heat-inactivated fetal bovine serum (Hyclone), 2 mM L-glutamine (Invitrogen), 100 U/ml penicillin and 100 μg/ml streptomycin (Invitrogen) in a humidified 37°C, 5% CO_2 tissue culture incubator. Transient transfections were performed using Genejuice transfection reagent (Novagen) in accordance with the manufacturer's directions for sub-confluent cells. MLN4924 was a gift from Millennium Pharmaceuticals, Inc.

Plasmid constructs

The FLAG- or V5-*B. pseudomallei* Cif plasmids bearing an N-terminal 2X FLAG or V5 epitope tag sequence used were previously described [12]. *B. pseudomallei* Cif C156S catalytic mutant (V5-Cif C156S) was generated via site-directed mutagenesis using forward primer 5'-GAT GAC GCC CGT GTC CGG ACT TTC GGC CA-3' and reverse primer 5'-TGG CCG AAA GTC CGG ACA CGG GCG TCA TC-3', and cloned into pcDNA3.1 with 5' KpnI and 3' XbaI and verified by DNA sequencing.

FLAG-Bim_{EL} plasmid was a kind gift from Dr. Ong Sin Tiong. pBabe-Puro-MEK-DD and pBabe-Puro-B-RAF-V600E were gifts from William Hahn (Addgene plasmid # 15268 and # 15269 respectively). The FLAG-WT HRas and FLAG-G12V HRas plasmids were generated by amplification from mEGFP-HRas and mEGFP-HRas G12V (Yasuda *et al*., 2006) (gifts from

Karel Svoboda, Addgene plasmid # 18662 and # 18666, respectively) and cloned into pcDNA3.1 with 5' KpnI and 3' XbaI as described above. FLAG-S17N HRas, dn SH2, SH3N (N-terminal SH3 domain) and SH3C (C-terminal SH3 domain) Grb2-HA plasmids were generated via site-directed mutagenesis and verified by DNA sequencing. FLAG-mSOS1 plasmid was a kind gift from Dr. Low Boon Chuan. FLAG-mSOS1 truncation mutants were generated by PCR through sequential C-terminal truncations.

To generate S1164A/S1196A and S1164D/S1196D SOS1 mutants, I used gene synthesis (ShineGene Molecular Biotech, Inc.) and ordered the mouse SOS1 gene sequences between an internal AatII restriction site (nucleotide 3433) and the stop codon, including nucleotide substitutions that result in the S1164A/S1196A and S1164D/S1196D mutations (sequences as indicated in Figure 3). The two synthesised gene sequences were inserted into the FLAG-SOS1 pcDNA3.1 plasmid using the internal AatII restriction site and the XbaI site located immediately 3' to the stop codon.

Gene synthesis

mSOS Ala Mutant

(mSOS1 S1164A/S1196A) (the mutated codons are indicated in capitals)

gacgtccagagtctgccccagctgaatcctccccatccaagattatgtctaagcacttggac**GCA**cccccagctattcctcctaggcaacccacatcc
AatII
aaagcctattcaccacgctattcaatatcagatcggacctctatatcagatcctcctgaa**GCA**cctcccttgttaccaccacgggaacctgtgaggac
acctgatgttttctcaagctcaccattacatctccaacctcctcctttgggcaaaaagagtgatcatggcaacgccttcttcccaaacagcccatccccctt
ttacaccgccaccccccccaaacccccctctcctcatggcacgagaaggcatctgccatcaccaccactgacacaggagatggacctccattccattgctg
ggcctcctgttcctccacgacaaagcacttctcaacttatccccaaactccctccaaaaacttacaaaagggagcacacacacccatccatgcataga
gatggaccaccactgctggagaatgcccattcttcctaa**tctaga**
Stop **XbaI**

mSOS Asp Mutant

(mSOS1 S1164D/S1196D) (the mutated codons are indicated in capitals)

gacgtccagagtctgccccagctgaatcctccccatccaagattatgtctaagcacttggac**GAC**cccccagctattcctcctaggcaacccacatcc
AatII
aaagcctattcaccacgctattcaatatcagatcggacctctatatcagatcctcctgaa**GAC**cctcccttgttaccaccacgggaacctgtgaggac
acctgatgttttctcaagctcaccattacatctccaacctcctcctttgggcaaaaagagtgatcatggcaacgccttcttcccaaacagcccatccccctt
ttacaccgccaccccccccaaacccccctctcctcatggcacgagaaggcatctgccatcaccaccactgacacaggagatggacctccattccattgctg
ggcctcctgttcctccacgacaaagcacttctcaacttatccccaaactccctccaaaaacttacaaaagggagcacacacacccatccatgcataga
gatggaccaccactgctggagaatgcccattcttcctaa**tctaga**
Stop **XbaI**

Figure 3. Generation of mouse SOS1 S1164A/S1196A and S1164D/S1196D mutants by gene synthesis.

Immunoblotting

Cells were washed with ice-cold Phosphate-Buffered Saline (PBS) and then lysed in Triton X-100-containing lysis buffer. The composition of the lysis buffer was as follows: 25 mM Tris-HCl (pH 7.5), 100 mM NaCl, 2.5 mM EDTA, 2.5 mM EGTA, 20 mM NaF, 1 mM Na_3VO_4, 20 mM Sodium β-Glycerophosphate, 10 mM Sodium Pyrophosphate, 0.5% Triton X-100, Roche protease inhibitor cocktail and 0.1% β-Mercaptoethanol. Lysates were

precleared by centrifugation before use for Western blotting. Equal amounts of protein were loaded for Western blot analysis. All the following antibodies used were obtained from Cell Signaling Technology: anti-phospho-p38 (Thr180/Tyr182), anti-p38, anti-phospho-SAPK/JNK (Thr183/Tyr185), anti-SAPK/JNK, anti-phospho-ERK1/2 (Thr202/Tyr204), anti-ERK1/2, anti-Mcl-1, anti-phospho-Bad (Ser112), anti-Bad, anti-phospho-MEK1/2, anti-MEK1/2, anti-Grb2, anti-phospho-Akt (Thr308), anti-Akt, anti-phospho-STAT3 (Tyr705), anti-STAT3, except for anti-p27 (BD Biosciences), anti-HIF-1α (BD Biosciences), anti-α-tubulin (Molecular Probes), anti-β-actin (Sigma), anti-FLAG M2 (Sigma), anti-V5 (Serotec) and anti-HA (Roche). All Western blots shown are representative of two independent experiments.

Immunoprecipitation

20 µl of anti-FLAG M2 agarose beads (Sigma) was used for immunoprecipitation. 500 µl of precleared lysate from cells transfected with FLAG-mSOS1 + empty vector or FLAG-mSOS1 + V5-Cif in 60-mm tissue culture dishes was added to the agarose beads. Untransfected cell lysate was added to control beads. The samples were tumbled for 1 hour at 4°C, and the beads were then washed four times in ice-cold NP40 lysis buffer (containing 50 mM NaCl, 0.5% NP-40, 5% glycerol, 0.5 mM EDTA, 50 mM Tris, pH 7.5) and once in ice-cold buffer containing 50 mM Tris (pH 7.5). The immunoprecipitated mSOS1 proteins were then eluted and denatured in 2X Laemmli sample buffer (Biorad) containing 5% β-Mercaptoethanol and subjected to SDS-PAGE and Western blotting.

3. RESULTS

3.1 Stabilisation of CRL substrates by Cif is dependent on its catalytic activity

It has been described that Cif catalyses the deamidation of NEDD8, and results in the stabilisation of CRL substrates such as p21 and p27 (Cui *et al*., 2010). Hence, in my Honours project, I first confirmed this report by examining the effect of Cif on the cellular abundance of some CRL substrates including p27 and HIF-1α in mammalian cells. I performed transient transfection of *cif* plasmid that was amplified from *B. pseudomallei* strain K96243 (Boh *et al*., 2011) in HEK 293T cells. MLN4924, the NEDD8 E1-activating enzyme inhibitor, was used as a positive control (Soucy *et al*., 2009). As shown in Figure 4A, Cif induced a marked accumulation of CRL substrates p27 and HIF-1α compared to the empty vector transfected cells. In contrast, Cif did not affect the stability of the non-CRL proteasome substrates cyclin B1 and geminin (Figure 4B). Similar to Cif transfected cells, MLN4924 treated cells also showed an increase in p27 and HIF-1α protein levels, but notably to a lesser extent than the effect of Cif. Therefore, Cif was shown to be more potent than MLN4924 in stabilising the CRL substrates p27 and HIF-1α.

To further validate that CRL substrate stabilisation by Cif is dependent on its deamidase activity, I constructed a catalytically inactive *cif* mutant as described by Yao *et al*. (2009). Using site-directed mutagenesis, I mutated the critical cysteine residue at position 156 in the catalytic domain to serine. As I would have expected, when this catalytic *cif* mutant (Cif C156S) was

expressed in cells, no significant difference in the cellular abundance of p27 was detected compared to control cells, whereas the wild type Cif was capable of inducing p27 accumulation (Figure 4C). This confirmed that the catalytic activity of Cif is indeed required to inhibit CRL function. When this activity is abolished, Cif is impaired in stabilising CRL substrates.

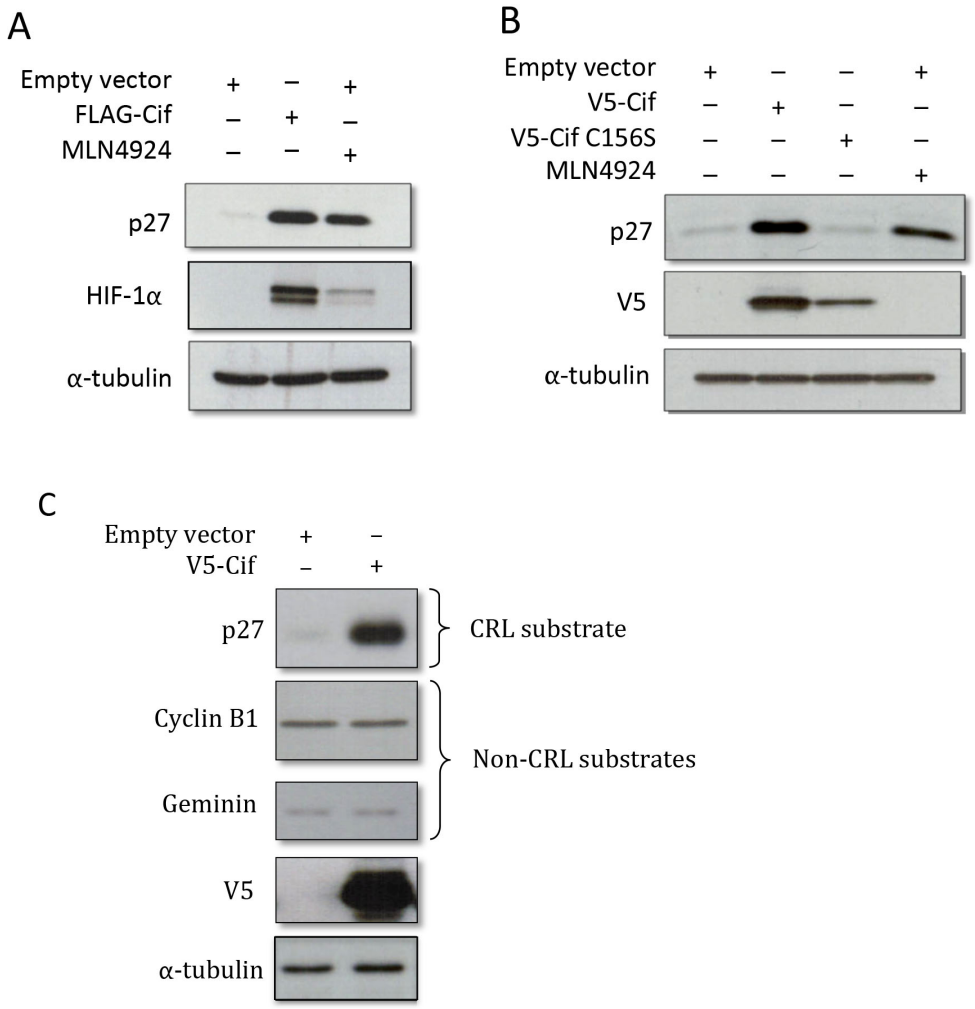

Figure 4. Effect of Cif on CRL substrates stabilisation. HEK 293T cells were transfected with *B. pseudomallei* Cif expression plasmids (either FLAG-tagged Cif or V5-tagged Cif or Cif C156S) for 48 hours and treated with 1 μM MLN4924 for the last 24 hours. Cell lysates were resolved using SDS-PAGE and cellular abundance of CRL and non-CRL substrates was analysed using Western blotting.

3.2 Cif increases ERK MAPK phosphorylation in a manner dependent on its deamidase activity but independent of CRL inhibition

In my efforts to discover mechanisms of action of Cif that are independent of CRL inhibition, I observed that Cif has a potent activating effect on the ERK pathway (see Figure 5B). Therefore, I sought to determine the exact molecular target and mechanism of action of Cif in regulating ERK activity. I first determined if Cif exhibits a preference for activating the ERK pathway compared to the p38 or SAPK/JNK MAPK pathways. Ectopic expression of Cif using a FLAG- or V5-epitope tagged Cif plasmid in HEK 293T cells resulted in a marked induction of ERK1/2 phosphorylation. In contrast, Cif caused only a slight increase in p38 and SAPK/JNK phosphorylation (Figure 5A and B). This indicates that Cif selectively and potently activates the ERK MAPK pathway.

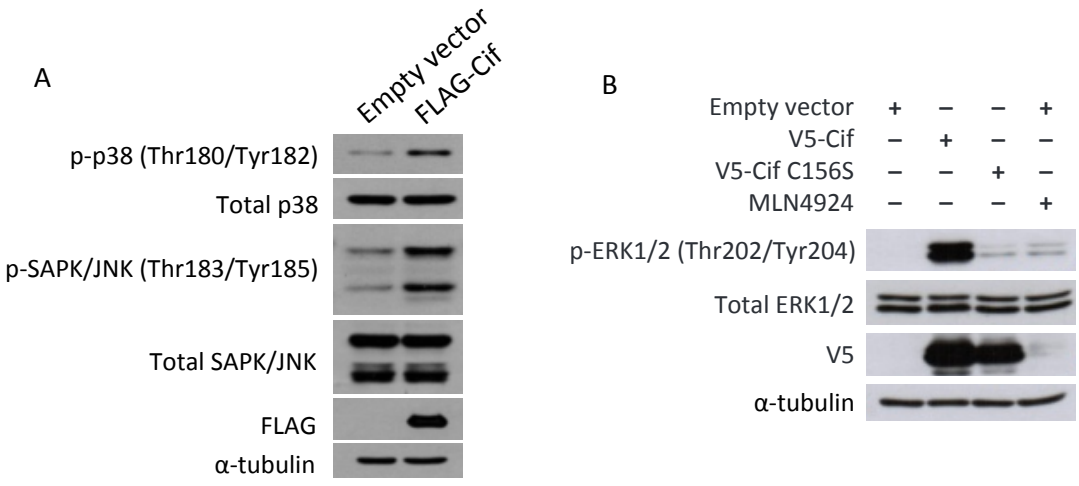

Figure 5. Cif specifically increases ERK MAPK phosphorylation. (A, B) HEK 293T cells were transfected with the indicated expression plasmids for 2 days, and in (B) treated with 1 μM MLN4924 for the last 24 hours. Pre-cleared cell lysates were then subjected to Western blotting analysis with the indicated antibodies.

Cif has recently been reported to function as a deamidase, and its deamidase activity is dependent on its catalytic triad (Cui *et al*., 2010). Hence, I next sought to determine if the effect of Cif on ERK phosphorylation is dependent on its deamidase activity. To test this, I expressed a mutant of Cif in which the catalytic cysteine 156 residue in the triad is mutated to serine (C156S), in cells. As shown in Figure 5B, the catalytic inactive Cif mutant did not increase ERK1/2 phosphorylation, suggesting that ERK activation by Cif is dependent on its deamidase activity. It was noted that the expression level of the Cif mutant is not identical to that of wild type Cif. Hence, to confirm that the lack of effect of the Cif mutant is not due to the lower expression level, I performed a titration of the Cif mutant and measured the level of ERK activation. I found that a dose-dependent increase in the expression of the Cif mutant did not result in a corresponding increase in ERK activation (Figure 6). This further supports the finding that the Cif mutant is impaired in activating ERK, and that the effect of Cif on ERK activation is dependent on its deamidase activity.

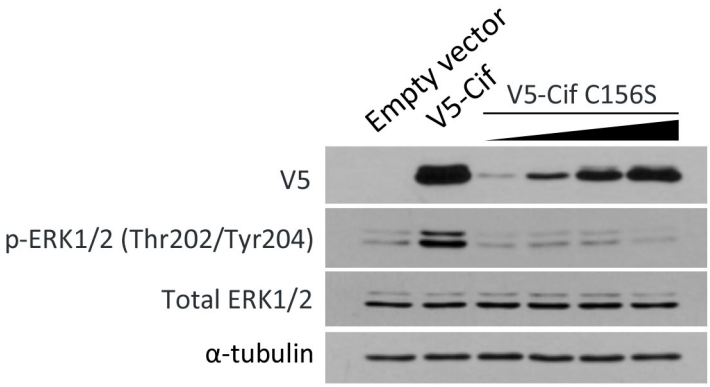

Figure 6. Cif increases ERK MAPK phosphorylation in a manner dependent on its deamidase activity. HEK 293T cells were transfected with the indicated expression plasmids. For V5-Cif C156S expression, increasing amounts were

transfected, with the lowest amount equal to that of V5-Cif expression plasmid. Cell lysates were analysed by Western blotting using the indicated antibodies.

To date, the only known mechanism of action of Cif is to inhibit CRL activity via deamidation of its substrate Nedd8 (Cui *et al*., 2010). Therefore, I investigated whether the effect of Cif on ERK activation is a consequence of CRL inhibition. To test this, I used the CRL inhibitor MLN4924. MLN4924 blocks the activation of Nedd8 by the Nedd8 E1-activating enzyme (Soucy *et al*., 2009). This prevents the transfer of Nedd8 onto CRLs and blocks the conformational change that is required to activate CRLs. As shown in Figure 5B, when cells were treated with MLN4924, no increase in ERK activation was observed. This suggests that ERK activation is unlikely to be a consequence of CRL inhibition. To confirm this result, I used an alternative approach to inhibit CRL activity by employing a cell line that expresses a dominant negative mutant of the Nedd8 E2-conjugating enzyme Ubc12 (dnUbc12). In this cell line, dnUbc12 expression is under control of a tetracycline-inducible promoter (Chew *et al*., 2007). Upon addition of tetracycline, dnUbc12 is induced and sequesters cellular Nedd8, thereby preventing endogenous Ubc12 from conjugating Nedd8 onto CRLs. As shown in Figure 7, expression of Cif resulted in a similar increase in ERK1/2 phosphorylation in the absence and presence of tetracycline (lane 2 and 4). Thus, Cif causes marked ERK activation even when CRL activity is inhibited. Similarly, when Cif was expressed in the presence of the CRL inhibitor MLN4924, a further increase in ERK activity was observed (compare lane 6 to lane 5 in Figure 7). Taken together, these results suggest that the effect of Cif

on ERK activity is independent of CRL inhibition, but dependent on Cif deamidase activity. Therefore, I hypothesised that Cif activates the ERK MAPK pathway *via* a target that is different from CRLs.

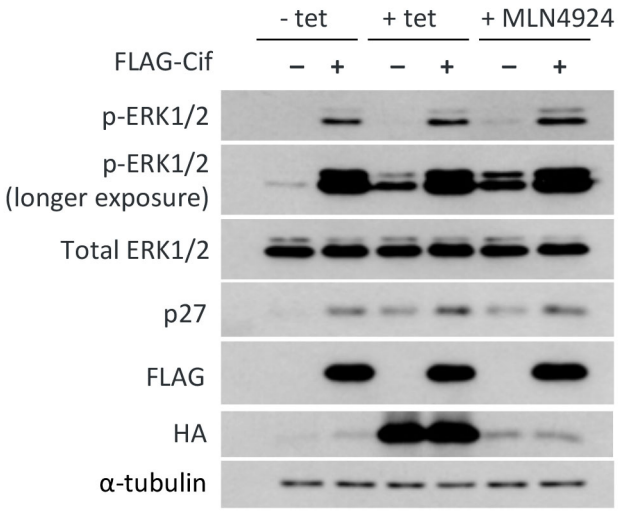

Figure 7. Cif increases ERK MAPK phosphorylation in a manner independent of CRL inhibition. Tetracycline-inducible dominant negative Ubc12 HEK293 cells were transfected with FLAG-Cif expression plasmid for two days. Cells were then either treated with 1 μM tetracycline to induce dnUbc12 expression for the last 24 hours or treated with 1 μM MLN4924 for the last 24 hours. Cell lysates were then analysed by Western blotting using the indicated antibodies.

3.3 ERK activation confers a pro-survival signal through phosphorylation of the pro-apoptotic protein Bim

It has been postulated that the inhibition of cell cycle progression as a result of Cif-dependent CRL inhibition slows down the turnover rate of epithelial cells (Kim *et al*., 2010; Taieb *et al*., 2011), thus promoting bacterial colonization of the lung epithelium. However, it is well known that prolonged CRL inhibition results in the accumulation of key cell cycle mediators and ultimately induction of cellular apoptosis (Soucy *et al*., 2009; Milhollen et al.,

2011). The induction of apoptosis would self-limit *B. pseudomallei* infection. This raises the question of how the bacterium simultaneously inhibits host cell proliferation and prevents cell apoptosis. Therefore, I hypothesised that the physiological role of Cif in activating the pro-survival ERK MAPK pathway is to counter the pro-apoptotic effects of CRL inhibition.

ERK is known to inhibit cellular apoptosis by regulating the phosphorylation status of the BH3 only protein Bim (Ley *et al.*, 2005). Therefore, I examined whether Cif functions to modulate Bim phosphorylation. There are three major isoforms of Bim that are generated as a result of alternative splicing: Bim short (Bim_S), Bim long (Bim_L), and Bim extra long (Bim_{EL}) (Ley *et al.*, 2005). Bim_{EL} has been reported to be the most abundant isoform. This isoform has also been shown to contain an ERK1/2 docking domain and ERK1/2 phosphorylation sites. Phosphorylation of Bim_{EL} by ERK1/2 targets it to the proteasome for degradation. Therefore, to test whether Cif counters the effect of the proapoptotic protein Bim, I expressed FLAG-tagged Bim_{EL} in the presence or absence of Cif and measured the phosphorylation of Bim_{EL} by western blot. I also used a known activator of ERK MAPK, active MEK (MEK-DD), as a positive control, as well as the MEK inhibitor U0126 as a negative control. As shown in Figure 8A, a band shift in Bim_{EL} was detected when FLAG-Bim_{EL} was co-expressed with Cif, compared to the empty vector control in the first lane. A similar band shift was also observed when FLAG-Bim_{EL} was co-expressed with MEK-DD. Cif- and MEK-DD-induced Bim_{EL} phosphorylation was not observed when ERK1/2 activation

by Cif and MEK-DD was prevented through treatment with U0126 (Figure 8B). This indicates that Cif-induced Bim_{EL} phosphorylation is dependent on MEK.

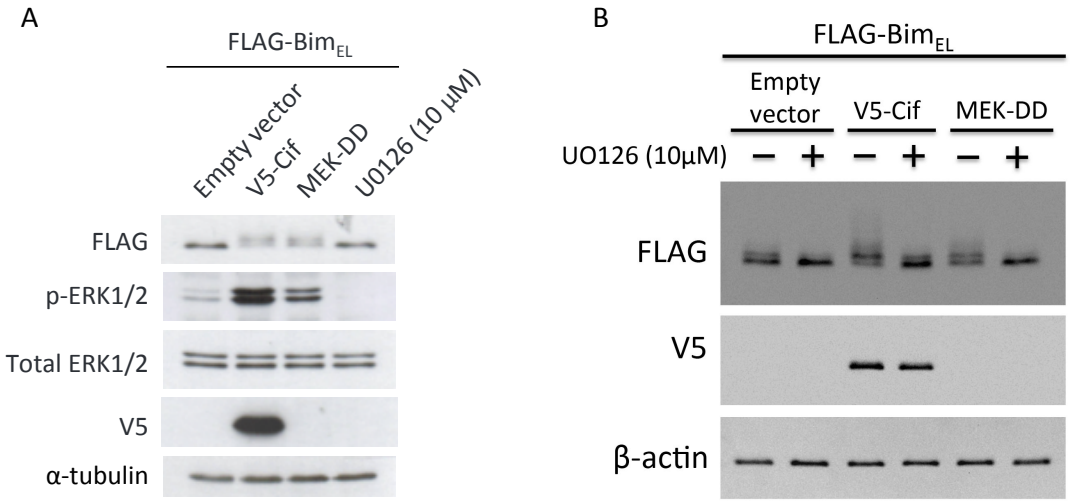

Figure 8. Cif regulates the expression of Bim_{EL}. (A) HEK 293T cells were co-transfected with FLAG-Bim_{EL} and V5-Cif, MEK-DD or empty vector, or treated with 10 μM U0126 for the last 6 hours. Cell lysates were then subjected to Western blotting using the indicated antibodies. (B) HEK 293T cells were co-transfected with FLAG-Bim_{EL} and V5-Cif, MEK-DD or empty vector and treated with 10 μM U0126 for the last 6 hours, as indicated, followed by Western blotting using the indicated antibodies.

Of note, I also observed that Cif expression increased the protein levels of anti-apoptotic Mcl-1 and promoted inhibitory phosphorylation of the pro-apoptotic Bad protein at Serine 112 (Figure 9). However, these effects of Cif were not inhibited by U0126 and were hence ERK1/2 independent. Moreover, inhibition of CRL activity with MLN4924 did not mimic the effects of Cif on Mcl-1 and Bad. Hence, the Cif induced increases in Mcl-1 protein expression and Bad Serine 112 phosphorylation are likely not due to CRL inhibition. Thus, when taken together my results suggest that Cif can exert anti-apoptotic effects through ERK1/2 dependent and independent

mechanisms. This may play a role to counter the pro-apoptotic effects of Cif dependent CRL inhibition.

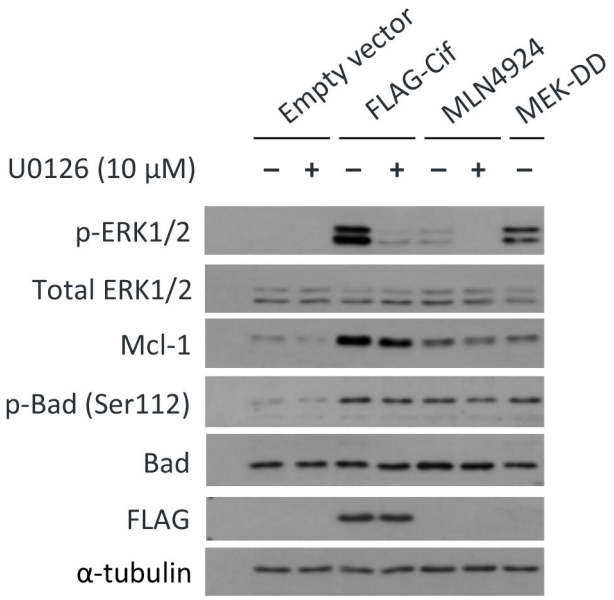

Figure 9. Cif regulates the expression or activity of apoptosis related proteins. HEK 293T cells were transfected with FLAG-Cif or empty vector and treated with 10 μM U0126 for the last 6 hours, as indicated, followed by Western blotting using the indicated antibodies.

3.4 Activation of the ERK MAPK pathway is independent of MAPK phosphatases but dependent on upstream kinases in the MAPK pathway

Cif could potentially induce ERK1/2 phosphorylation via two mechanisms – by inhibiting MAPK phosphatases or by activating ERK or upstream MAP kinases. To first determine if Cif induces ERK activation by inhibiting the MAPK phosphatases, I treated cells with the phosphatase inhibitor okadaic acid and measured ERK phosphorylation in the presence or absence of Cif. If Cif activates ERK by inhibiting MAPK phosphatases, it

would be expected that Cif has less effect in cells in which MAPK phosphatases have been inactivated through okadaic treatment. However, as shown in Figure 10A, expression of Cif resulted in a similar increase in ERK phosphorylation in the absence and presence of okadaic acid. Thus, Cif increases ERK phosphorylation even when MAPK phosphatases are inhibited. This suggests that Cif-induced ERK activation is mediated via a mechanism that is different from MAPK phosphatase inhibition.

However, in the experiment in Figure 10A, okadaic acid was only present during the last hour due to cytotoxic effects. Furthermore, I noted that okadaic acid treatment only resulted in a slight increase in ERK phosphorylation under basal conditions, suggesting that okadaic acid may not potently inhibit MAPK phosphatases (compare lane 3 to 1). Hence, to confirm that Cif activates the ERK pathway via a mechanism that is independent of MAPK phosphatase inhibition, I performed a chase experiment whereby I followed the rate of ERK dephosphorylation in the presence of the MEK inhibitor U0126. U0126 blocks the activity of phosphorylated MEK, thus rendering MEK unable to phosphorylate downstream ERK1/2. Hence, under these conditions, Cif would be expected to be unable to induce ERK1/2 phosphorylation and could only increase ERK1/2 steady state phosphorylation levels by inhibiting the activity of a phosphatase that dephosphorylates ERK. In the experiment in Figure 10B, ERK1/2 phosphorylation was induced by transfecting cells with either Cif or constitutively active B-Raf-V600E. At time zero, cells were treated with U0126 to prevent further ERK1/2 phosphorylation. As shown in Figure 10B, in cells expressing B-Raf-V600E,

treatment with U0126 resulted in a decrease in ERK1/2 phosphorylation over time. In cells transfected with Cif, ERK1/2 dephosphorylation was not inhibited. This indicates that Cif does not function by inhibiting the activity of a phosphatase that dephosphorylates ERK. ERK1/2 phosphorylation did in fact decrease significantly faster in Cif-transfected cells compared to control cells. The reason for this is currently not clear. In summary, the results suggest that it is unlikely that Cif functions by inhibiting MAPK phosphatases to prevent ERK dephosphorylation.

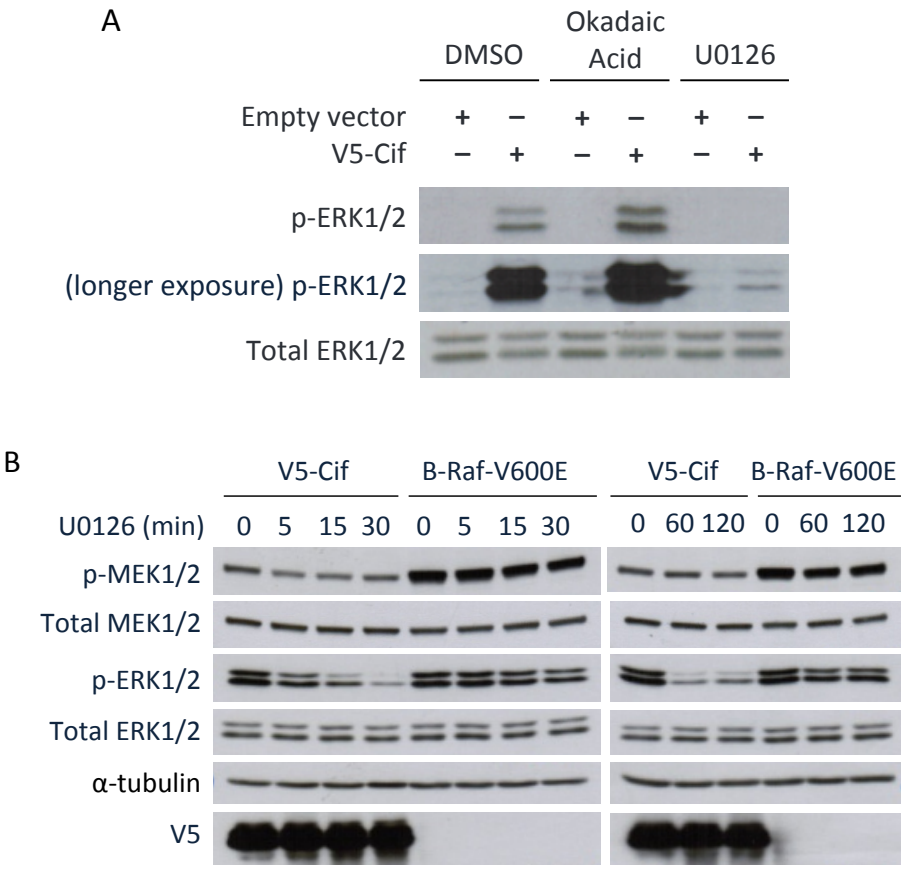

Figure 10. Cif activates ERK MAPK signaling in a manner independent of MAPK phosphatases but dependent on MAPK kinases. (A) HEK 293T cells were transfected with V5-Cif or empty vector and treated with 20 nM okadaic acid, 10 μM U0126 or 0.1% DMSO control for the last hour. Cells were then lysed and analysed by Western blotting using the indicated antibodies. (B) HEK 293T cells were transfected with V5-Cif or B-Raf-V600E and treated with 10 μM U0126 for the last 5

to 120 minutes, followed by Western blotting of the cell lysates using the indicated antibodies.

3.5 Cif targets the ERK MAPK pathway upstream of Ras and downstream of RTKs

To elucidate the target of Cif in the ERK MAPK pathway, I took a systematic bottom-up approach. Thus, I examined if Cif directly activates a candidate kinase or a kinase that is upstream in the pathway by using a panel of kinase inhibitors (Figure 11A). In this pathway, ERK is a downstream target of the ERK kinase (MEK1/2). MEK1/2 is activated by an upstream serine/threonine kinase Raf. Raf is in turn regulated by the small GTPase Ras, which is an effector of the tyrosine kinase epidermal growth factor receptor (EGFR). I found that when cells were treated with the MEK inhibitor U0126, Cif-dependent ERK activation was completely prevented (Figure 9, Figure 10A – compare lane 6 to 2). U0126 blocks the ability of active MEK to phosphorylate ERK1/2. Therefore, the lack of effect of Cif on ERK phosphorylation in the presence of U0126 suggests that Cif does not directly activate ERK but functions upstream of the ERK kinase.

I next determined whether Cif directly activates MEK or another kinase or signaling intermediate that is further upstream of MEK. I treated cells with the Raf inhibitor BAY 43-9006, which inhibits the kinase activity of C-Raf and B-Raf and thus blocks MEK and ERK phosphorylation. As shown in Figure 11B, inhibition of Raf activity with BAY 43-9006 significantly inhibited activation of ERK by Cif (compare lane 4 to 2), suggesting that it is unlikely

that Cif directly activates MEK. This result indicates that Cif may mediate its effect on ERK activation via Raf or a target that is upstream of Raf.

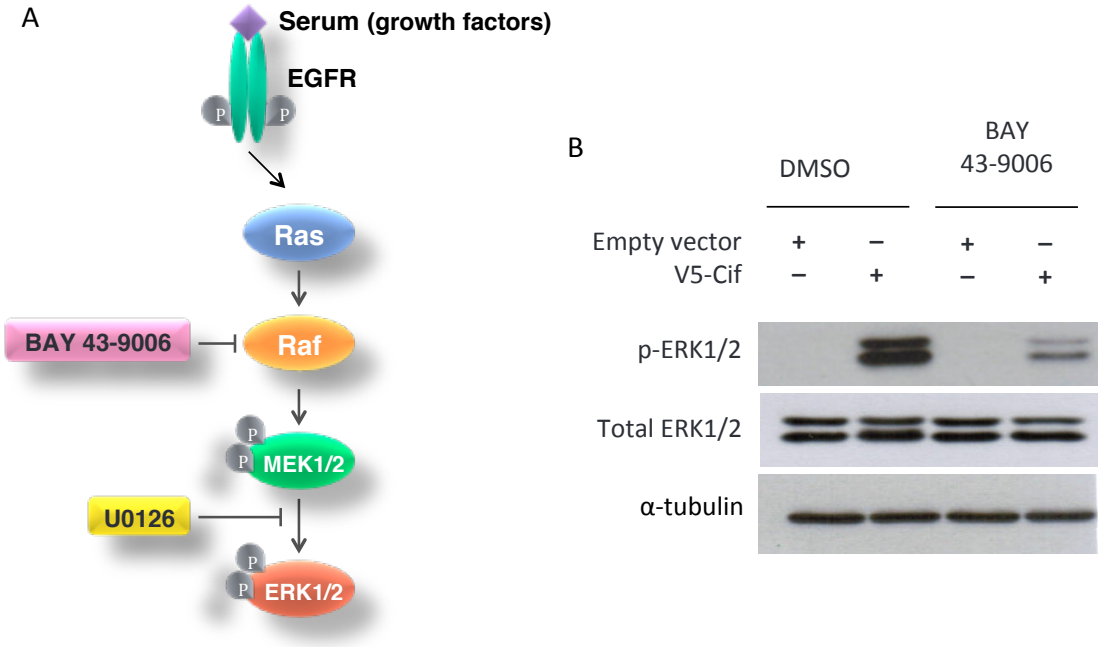

Figure 11. Cif likely activates Raf or a target that is upstream of Raf. (A) Schematic diagram of ERK/MAPK pathway. (B) HEK 293T cells were transfected with the indicated expression plasmids for two days and then treated with 10 μM BAY 43-9006 or 0.1% DMSO for the last 6 hours, followed by Western blotting of the cell lysates using the indicated antibodies.

Therefore, to determine if Cif directly activates Raf, I used a dominant negative Ras mutant, S17N HRas, as an approach to inhibit Ras activity. It is generally accepted that S17N HRas exerts its effects by sequestering upstream activators and simultaneously being impaired in activating downstream effectors (Nassar *et al.*, 2010). As a result, S17N HRas inhibits the activation of endogenous Ras and prevents downstream Ras signaling events. When I expressed FLAG-tagged S17N HRas, I observed that the dominant negative Ras completely blocked the effect of Cif on ERK activity

(Figure 12 – compare lane 4 to 2). This result suggests that Cif functions at the level of Ras or upstream of Ras to mediate its effect on ERK activation.

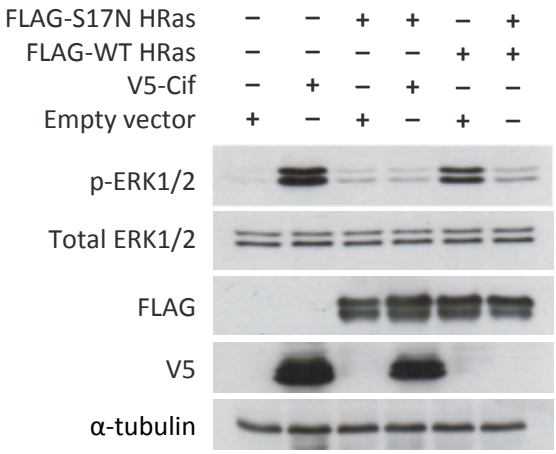

Figure 12. Cif likely activates ERK MAPK signaling at the level of Ras or upstream of Ras. HEK 293T cells were transfected with the indicated expression plasmids for two days, followed by Western blotting of the cell lysates using the indicated antibodies.

The dominant negative Ras functions by sequestering the upstream Grb2-SOS1 complex. This suggests that ERK activation by Cif is dependent on a functional Grb2-SOS1 complex. In response to RTK activation, the Grb2 protein normally recruits SOS1 to the plasma membrane. Upon plasma membrane translocation, SOS1 can activate plasma membrane-bound Ras by functioning as a guanine nucleotide exchange factor (GEF) for Ras. Therefore, we next tested whether Cif requires plasma membrane translocation of the Grb2-SOS1 complex to activate ERK. To test this, I used dominant negative mutants of Grb2 that prevent the recruitment of SOS to the plasma membrane (Tanaka *et al.*, 1995; Gupta and Mayer, 1998). The Grb2 protein contains two Src Homology 3 (SH3) domains, one at the N-terminus

and the other at the C-terminus of Grb2. The SH3 domains mediate the binding to a proline-rich region in SOS. The Grb2 protein also contains one Src Homology 2 (SH2) domain that is responsible for binding to specific phosphorylated tyrosine residues on activated RTKs. In our experimental approach, I used dominant negative SH2 and SH3 Grb2, in which the SH2 domain and the SH3 domains in Grb2 are inactivated by point mutations, respectively. Dn SH2 Grb2 is expected to bind to endogenous SOS1, but is unable to recruit SOS1 to RTKs. Hence, dn SH2 Grb2 sequesters SOS1 in the cytoplasm. In contrast, dn SH3 Grb2 is expected to bind to RTKs but not to SOS1. Consequently, dn SH3 Grb2 prevents binding of the endogenous Grb2-SOS1 complex to RTKs. As shown in Figure 13, when I co-expressed dn SH3N Grb2 (N-terminal) or dn SH3C Grb2 (C-terminal) with Cif, Cif-induced ERK activation was markedly inhibited, as indicated by the pronounced decrease in ERK phosphorylation (compare lane 6 or 8 to lane 2). This result suggests that the effect of Cif on the ERK MAPK pathway is dependent on the recruitment of SOS1 to the RTK.

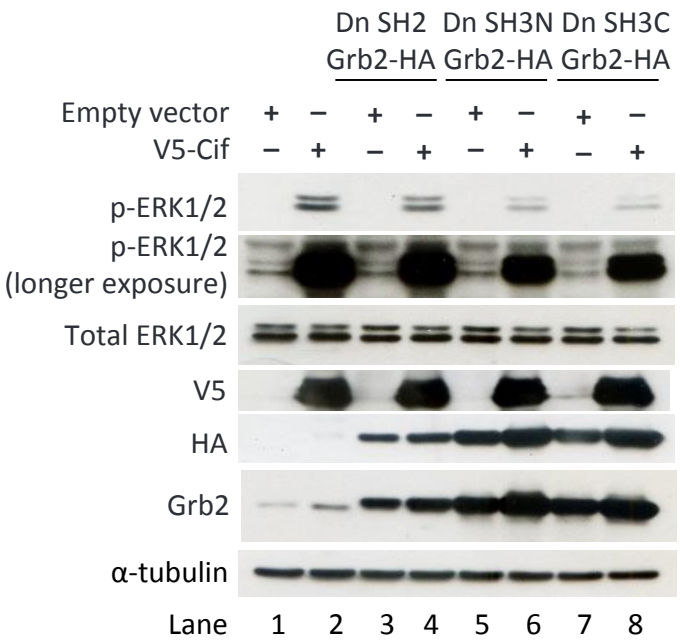

Figure 13. Cif-induced activation of MAPK/ERK signaling is dependent on a functional Grb2-SOS1 complex. HEK 293T cells were transfected with the indicated expression plasmids for two days, followed by Western blotting of the cell lysates using the indicated antibodies.

The dn SH2 Grb2 also inhibits the translocation of SOS1 to the plasma membrane. However, when I expressed dn SH2 Grb2, I only observed a slight inhibition of ERK activation by Cif (Figure 13, compare lane 4 to 2). It was noted, however, that compared to the dn SH3 Grb2 mutants, the expression level of dn SH2 Grb2 was lower. I thus tried to validate the dn Grb2 proteins by measuring their effects on growth factor-induced ERK1/2 activation. I found that dn SH3N Grb2 and dn SH3C Grb2 had a strong inhibitory effect, whereas dn SH2 Grb2 inhibited serum-induced ERK1/2 activation only weakly (Figure 14). Hence, the effect of the various dn Grb2 constructs on growth factor-induced ERK1/2 activation correlates well with their effects on Cif-induced ERK1/2 activation. Thus, taken together, my results suggest that ERK is

activated by Cif, presumably dependent upon the recruitment of the Grb2-SOS1 complex to the plasma membrane.

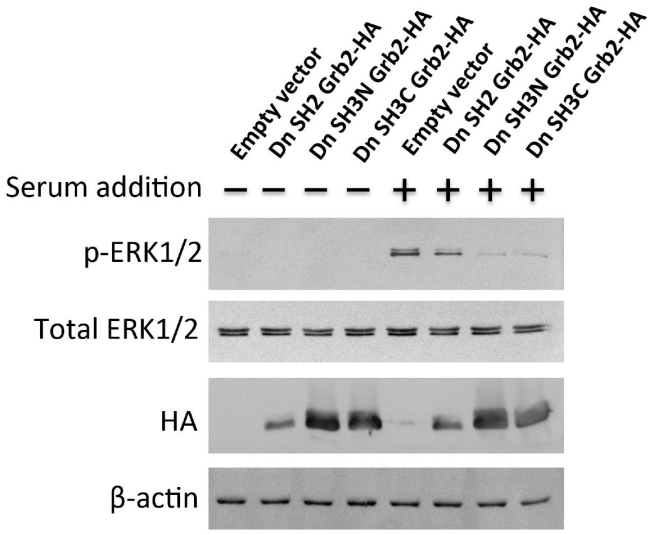

Figure 14. Effect of dominant negative Grb2 proteins on growth factor-induced ERK1/2 activation. HEK 293T cells were transfected with the indicated expression plasmids for two days. The cells were then incubated for 6.5 hours in serum free medium, followed by re-addition of serum for 30 min, where indicated. The cell lysates were then analysed by Western blotting using the indicated antibodies.

My results in Figure 13 raise the possibility that Cif functions by mediating RTK activation. To test this possibility, I examined the effect of Cif on the PI3K/Akt pathway, which is also downstream of RTKs. I found that Cif had no effect on the PI3K/Akt pathway as indicated by a lack of an increase in Akt phosphorylation at threonine 308 (Figure 15A). It is also known that growth factor signaling via RTKs can lead to the activation of the STAT3 pathway. However, I found that Cif transfection did not lead to STAT3 activation, as indicated by the lack of an increase in STAT3 phosphorylation at tyrosine 705, compared to the known activator of the STAT3 pathway

constitutively active Ras (G12V HRas) (Figure 15B). These results indicate that Cif does not directly activate RTKs and suggest that Cif targets the Grb2-SOS1 complex downstream of RTKs to activate the ERK MAPK pathway.

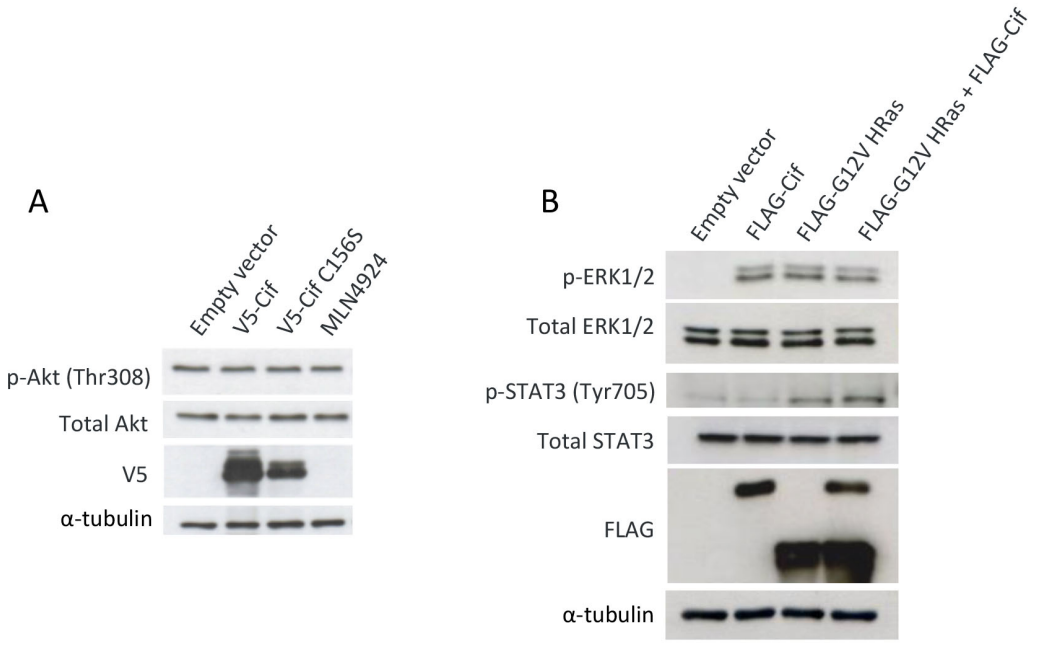

Figure 15. Cif likely activates ERK MAPK signaling at the level of the Grb2-SOS1 complex. (A, B) HEK 293T cells were transfected with the indicated expression plasmids for 2 days, and then treated with 1 μM MLN4924 (A) for the last 24 hours, followed by Western blotting of the cell lysates using the indicated antibodies.

3.6 Cif expression modifies SOS1 in a region containing the CDC25-H and proline-rich domains

My results suggest that Cif exerts its effects on the ERK MAPK pathway downstream of the RTKs, and that it potentially acts at the Grb2-SOS1 complex. Hence, I sought to characterise the potential mechanism through which Cif modifies the Grb2-SOS1 complex to activate ERK MAPK. Grb2-dependent recruitment of SOS1 to RTKs is required to activate the GEF

activity in SOS1 to catalyse GDP to GTP exchange in Ras (Groves and Kuriyan, 2010). I hence hypothesised that Cif increases Grb2-SOS1 binding to promote SOS1 activity. Therefore, I examined the binding of Grb2 to SOS1 in the presence or absence of Cif by using co-immunopreciptation. As shown in Figure 16, I was able to readily detect an interaction between transfected FLAG-SOS1 and endogenous Grb2. However, I found that there was no noticeable difference in the amount of Grb2 that was co-immunoprecipitated with SOS1 when Cif was present. This suggests that Cif does not alter Grb2-SOS1 binding to promote SOS1 activity. However, interestingly, I noted that the co-expression of SOS1 and Cif resulted in a slight band shift in SOS1 as seen in both the lysate and the FLAG IP lanes (Figure 16), suggesting that Cif may possibly induce SOS1 phosphorylation.

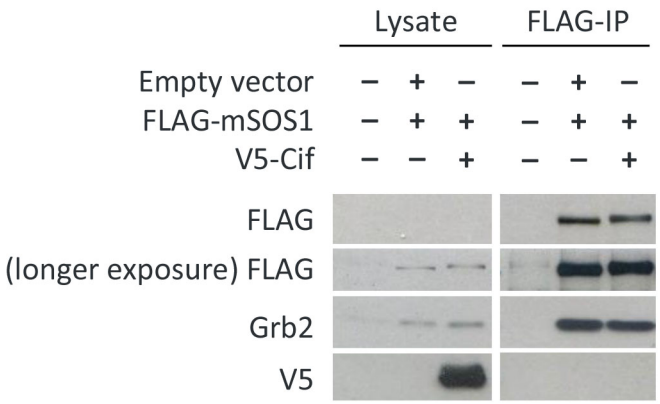

Figure 16. Cif does not alter Grb2-SOS1 but decreases mSOS1 mobility. HEK 293T cells were transfected with the indicated expression plasmids for two days, followed by FLAG immunoprecipitation from the cell lysates using FLAG-agarose, and subsequently Western blotting using the indicated antibodies.

The Ras guanine nucleotide exchange factor SOS1 has a multi-domain structure. The domain organisation of SOS1 comprises of a histone fold

domain, a Dbl homology (DH)-Pleckstrin homology (PH) domain, a Ras exchanger motif (REM), a CDC25-homology (CDC25-H) domain with GEF activity, and a proline-rich C-terminal region that binds Grb2 and links SOS1 to activated RTKs. The catalytic REM and CDC25-H domains govern the GEF activity of SOS1 on its target Ras protein. The histone fold domain and the DH-PH domain have been suggested to exert an auto-inhibitory effect on the catalytic REM and CDC25-H domains (Corbalan-Garcia *et al*., 1998; Rojas *et al.,* 2011). It is also known that the C-terminal proline-rich region of SOS1 contains multiple phosphorylation sites that possibly play a role in the regulation of Ras activation by SOS1 (Douville and Downward, 1997).

Given the key role of these domains in the regulation of SOS1 function, I therefore hypothesised that Cif modulates the phosphorylation status of one of these domains to contribute to increased ERK activation. To investigate and map the phosphorylation sites, I generated a number of mouse SOS1 (mSOS1) C-terminal deletion constructs comprising amino acids 1-1230, 1-757, and 1-574. I then co-expressed each deletion mutant with Cif to examine which region of SOS1 is responsible for the band shift in the presence of Cif. I found that only the mSOS1 (a.a 1-1230) mutant retained the band shift pattern similar to full length mSOS1 with Cif co-expression (Figure 17). In contrast, all other deletion constructs showed no band shift in the presence of Cif. This suggests that Cif likely modulates the phosphorylation status of mSOS1 in the region between amino acids 757 and 1230, which contains the CDC25-H and proline-rich domains.

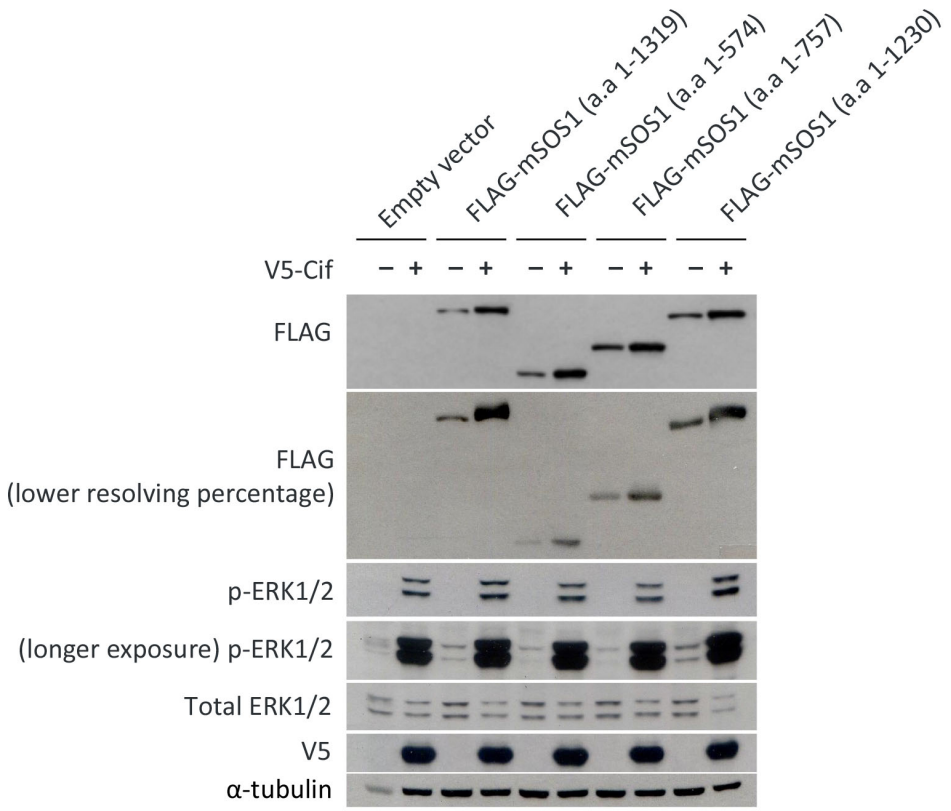

Figure 17. Cif expression regulates the CDC25-H and proline-rich domains in SOS1. HEK 293T cells were transfected with the indicated FLAG-mSOS1 truncation constructs for two days, followed by Western blotting using the indicated antibodies. The blot in the second panel was obtained from running a duplicate set of lysates through another SDS-PAGE gel of a lower resolving power.

To confirm that the Cif-induced slower migration of SOS1 is indeed due to phosphorylation, I used phosphatase treatment. In this approach, cell lysate was incubated with Calf Intestinal Alkaline Phosphatase (CIP) followed by SDS-PAGE and Western blotting to determine if the SOS1 mobility shift can be reversed. To validate this approach, I initially confirmed dephosphorylation of the known phosphoprotein FRAT1. As shown in Figure 18, transfected FRAT1-FLAG exhibits both basal phosphorylation (as indicated by the smear above the FRAT1-FLAG band in lane 1) as well as phosphorylation induced

by co-expression of GSK3β (see the mobility shift in lane 2). Both basal and GSK3β induced FRAT1 phosphorylation were reversed after incubation of the cell lysates with CIP.

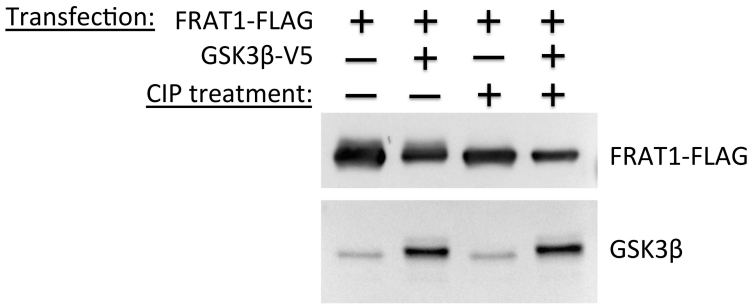

Figure 18. CIP-mediated FRAT1 dephosphorylation. HEK 293T cells were transfected with FRAT1-FLAG and GSK3β-V5 expression plasmids, as indicated. After two days, cells were lysed using triton X-100 lysis buffer that did not contain phosphatase inhibitors. Cell lysates were incubated with Calf Intestine Alkaline Phosphatase (CIP) (New England Biolabs) for one hour at 37°C (20 µl cell lysate with or without 20 units CIP). The reaction was stopped by adding 2xSDS loading buffer and the samples were analysed by SDS-PAGE and Western blotting. (NB: Transfected GSK3β-V5 in lanes 2 and 4 has a slightly increased size compared to endogenous GSK3β due to the presence of the V5 epitope tag.)

I then co-expressed SOS1 with or without Cif and determined if incubation of cell lysate with CIP was able to reverse the Cif-induced bandshift. However, in contrast to FRAT1, CIP did not reverse the bandshift of SOS1 (Figure 19). I also used Shrimp Alkaline Phosphatase, which was similarly unable to increase SOS1 mobility (data not shown). These results suggest that the Cif-induced phosphorylation sites are not dephosphorylated by Alkaline Phosphatases or alternatively that Cif induces a different type of post-translational modification in SOS1. However, these results also do not rule out Cif-induced phosphorylation on SOS1 as a plausible post-translational

modification because not all phosphorylated sites are sensitive to calf intestinal or shrimp alkaline phosphatases.

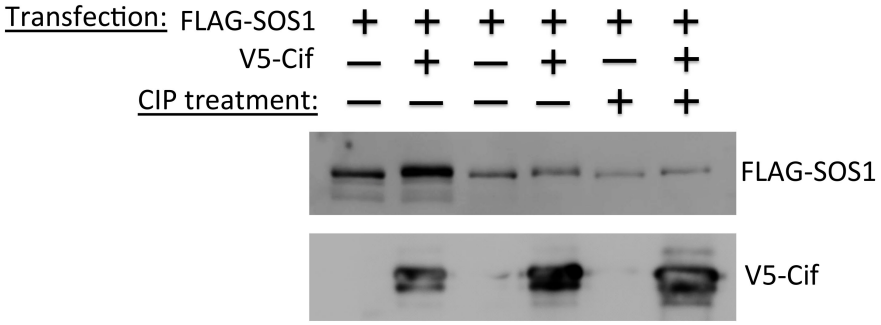

Figure 19. CIP-dependent SOS1 dephosphorylation. HEK 293T cells were transfected with FLAG-SOS1 and V5-Cif expression plasmids, as indicated. Cell lysis and Calf Intestine Alkaline Phosphatase (CIP) incubation were performed as described in Figure 5C. Lanes 1 and 2 correspond to the original lysates before the incubation at 37°C with or without CIP.

Therefore, I subsequently used an alternative mass spectrometry-based approach to determine whether Cif induces phosphorylation or other post-translational modifications in SOS1. Thus, I transfected three 15 cm-diameter petri dishes each with FLAG-mSOS1 with or without V5-Cif. Cells were then lysed and subjected to FLAG-immunoprecipitation. The FLAG immunoprecipitates were run on a 10% SDS-PAGE gel and the Coomassie-stained FLAG-mSOS1 bands (Figure 20) were excised, subjected to in-gel trypsin digestion and submitted for LC-MS/MS analysis by the NUS Protein and Proteomics Centre (PPC). The detected mSOS1 tryptic peptides were then analysed for differences in phosphorylation or other post-translational modifications in the presence or absence of Cif (Table 1).

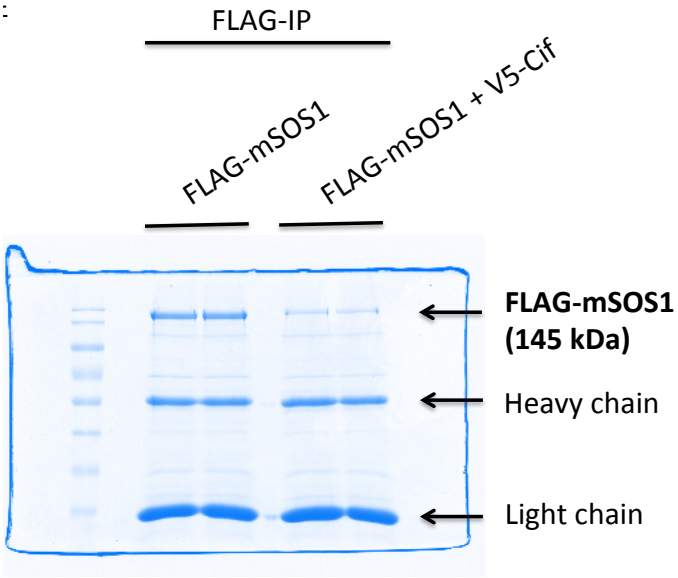

Figure 20. SOS1 immunopurification for mass spectrometry analysis. HEK 293T cells were transfected with the indicated expression plasmids for two days, and the cells were then lysed and subjected to FLAG-immunoprecipitation. The FLAG immunoprecipitates were run on a 10% SDS-PAGE gel (duplicate lanes for each sample), followed by staining of the gel using Coomassie Brillant Blue R-250. The FLAG-mSOS1 duplicate bands were excised and pooled together respectively, and subjected to in-gel trypsin digestion. The tryptic peptides were then analysed using LC-MS/MS by the NUS PPC. Shown here is a Coomassie gel image representative of three replicates.

Peptide sequence	Phosphorylation site in protein	No. of phosphorylated to unphosphorylated peptides (%)	
		Presence of Cif	Absence of Cif
LPGA**S**SAEYR	S484	1/22 (5%)	1/15 (7%)
IPESETESTASAPN**S**PR	S1082	3/6 (50%)	5/40 (13%)
TPL**T**PPPASGTSSNTDVCSVFDSDHSASPFHSR	T1088	1/11 (9%)	4/14 (29%)
SA**S**VSSISLSK	S1120	3/16 (19%)	4/17 (24%)
SASVS**S**ISLSK	S1123	1/16 (6%)	-
RPESAPAES**S**PSKIMSK	S1152	1/24 (4%)	4/21 (19%)
R(RPESAPAE**S**SPSKIMSK)	S1153	19/24 (79%)	12/21 (57%)
HLD**S**PPAIPPR(QPTSK)	S1164	40/50 (80%)	19/62 (31%)
TSISDPPE**S**PPLLPPR(EPVR)	S1196	24/28 (86%)	11/61 (18%)
TPDVF**S**SSPLHLQPPPLGK	S1213	-	2/72 (3%)
TPDVFSS**S**PLHLQPPPLGK	S1215	8/28 (29%)	1/72 (1%)
K(SDHGNAFFPNSPSPFTPPPPQ**T**PSPHGTR)(R)	T1249	-	1/18 (6%)
K(SDHGNAFFPNSPSPFTPPPPQTP**S**PHGTR)	S1251	1/12 (8%)	3/18 (17%)
R(HLP**S**PPLTQEM)(DLHSIAGPPVPP)(R)	S1261	32/39 (82%)	34/53 (64%)
HLPSPPL**T**QEMDLHSIAGPPVPPR	S1265	2/39 (5%)	1/53 (2%)

Table 1. Phosphorylation status of mSOS1 in the presence or absence of Cif. Phosphorylation sites detected in LC-MS/MS are indicated in red. Two candidate phosphorylated serine residues Ser1164 and Ser1196 (highlighted in green) showed higher tendency to be phosphorylated in the presence of Cif compared to in the absence of Cif and lie proximal to a PxxPxR motif. Trends observed in the LC-

MS/MS output shown in this table are representative of 2 separate experiments. "-": refers to no tryptic peptides detected. "()": refers to trypsin cut sites.

We identified two amino acids in mouse SOS1, Ser1164 and Ser1196, which showed increased phosphorylation in the presence of Cif. These residues are conserved in human SOS1 (Figure 21). Interestingly, these two serine residues are immediately proximal to two of the four proline-rich PxxPxR motifs in SOS1 (Figure 21). These motifs are involved in binding of SOS1 to the SH3 domain of Grb2, although a recent report found that they are not required for SOS1 interaction with Grb2 *in vivo* (Bartelt *et al*., 2015). Both of these serines in human SOS1 have been previously identified in a large-scale phosphoproteomics study and found to be phosphorylated residues (Zhou *et al*., 2013). However, there are no reports on the functional role of the phosphorylation of Ser1164 and Ser1196 or Ser1178 and Ser1210 in mouse or human SOS1, respectively.

***M. musculus* SOS1 (NP_033257)**

```
MEKEFTDYLF NKSLEIEPRH PKPLPRFPKK YSYPLKSPGV RPSNPRPGTM
      1060       1070       1080       1090       1100
RHPTPLQQEP RKISYSRIPE SETESTASAP NSPRTPLTPP PASGTSSNTD
      1110       1120       1130       1140       1150
VCSVFDSDHS ASPFHSRSAS VSSISLSKGT DEVPVPPPVP PRRRPESAPA
      1160       1170       1180       1190       1200
ESSPSKIMSK HLDSPPAIPP RQPTSKAYSP RYSISDRTSI SDPPESPPLL
      1210       1220       1230       1240       1250
PPREPVRTPD VFSSSPLHLQ PPPLGKKSDH GNAFFPNSPS PFTPPPPQTP
      1260       1270       1280       1290       1300
SPHGTRRHLP SPPLTQEMDL HSIAGPPVPP RQSTSQLIPK LPPKTYKREH
      1310
THPSMHRDGP PLLENAHSS
```

***H. sapiens* SOS1 (NP_005624)**

```
MEKEFTDYLF NKSLEIEPRN PKPLPRFPKK YSYPLKSPGV RPSNPRPGTM
      1060       1070       1080       1090       1100
RHPTPLQQEP RKISYSRIPE SETESTASAP NSPRTPLTPP PASGASSTTD
      1110       1120       1130       1140       1150
VCSVFDSDHS SPFHSSNDTV FIQVTLPHGP RSASVSSISL TKGTDEVPVP
      1160       1170       1180       1190       1200
PPVPPRRRPE SAPAESSPSK IMSKHLDSPP AIPPRQPTSK AYSPRYSISD
      1210       1220       1230       1240       1250
RTSISDPPES PPLLPPREPV RTPDVFSSSP LHLQPPPLGK KSDHGNAFFP
      1260       1270       1280       1290       1300
NSPSPFTPPP PQTPSPHGTR RHLPSPPLTQ EVDLHSIAGP PVPPRQSTSQ
      1310       1320       1330
HIPKLPPKTY KREHTHPSMH RDGPPLLENA HSS
```

Figure 21. C-terminal amino acid sequence of mouse and human SOS1. The identified Cif-induced phosphorylation sites are indicated in red and the PxxPxR motifs in SOS1 in bold.

3.7 Characterisation of the identified Cif-induced phosphorylation sites on SOS1

In order to characterise the functional significance of the Cif induced phosphorylation of SOS1 at Ser1164 and Ser1196, I generated a double mutant in which both serine residues were substituted with alanine, as described under Materials and Methods. I also generated an aspartate double substitution construct, which may potentially function as a phosphomimic mutant.

I first determined whether Cif induced SOS1 phosphorylation is prevented in the S1164A/S1196A mutant. Cells were transfected with wild type or mutant SOS1 with or without co-transfection of Cif. As shown in Figure 22, co-transfection of Cif induces an obvious decrease in wild type SOS1 mobility. When Cif was co-transfected with S1164A/S1196A mutant SOS1, the mobility shift was reduced. This result confirms that Cif induces SOS1 phosphorylation of Ser1164 and Ser1196 and suggests that phosphorylation of Ser1164 and/or Ser1196 is partially responsible for the observed slower migration of SOS1 when Cif is expressed.

I also determined whether expression of the non-phosphorylatable S1164A/S1196A SOS1 mutant inhibits Cif-dependent ERK1/2 activation. As shown in Figure 22, S1164A/S1196A mutant SOS1 was without effect on ERK1/2 activation by Cif.

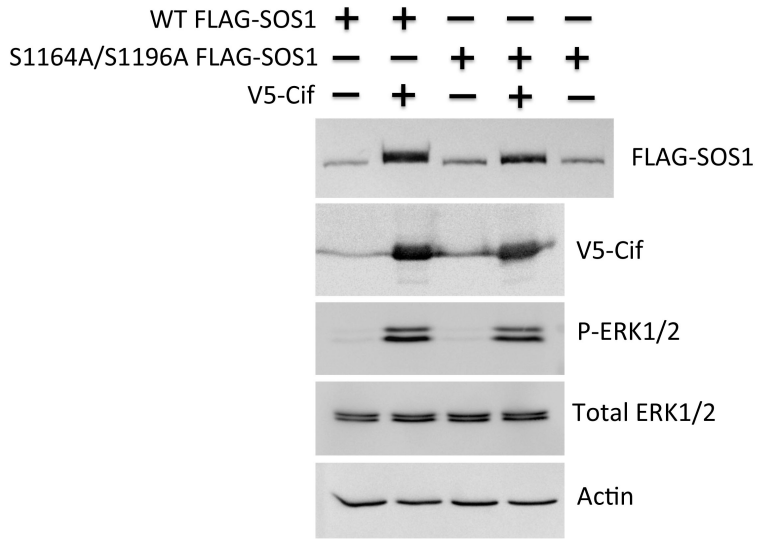

Figure 22. Characterisation of the identified Cif-induced phosphorylation sites on SOS1. HEK 293T cells were transfected with the indicated expression plasmids. Cell lysates were subjected to Western blotting with the indicated antibodies. Please

note that in the FLAG Western blot the “S1164A/S1196A SOS1, without V5-Cif” sample was run twice to better visualise the Cif-induced mobility shift.

I finally determined whether expression of the S1164D/S1196D SOS1 mutant mimics Cif-dependent ERK activation. To this end, I transfected cells with empty vector, wild type, S1164A/S1196A or S1164D/S1196D mutant SOS1 and determined the effect on ERK1/2 activity. As shown in Figure 23, overexpression of wild type SOS1 increased ERK1/2 phosphorylation. The S1164A/S1196A mutant had a similar effect on ERK1/2 phosphorylation compared to wild type SOS1. The S1164D/S1196D mutant did not further increase ERK1/2 activity compared to the effect exerted by wild type SOS1. This suggests that the S1164D/S1196D is unable to mimic the effect of Cif on the MAPK/ERK pathway. Taken together, the results indicate that Cif indeed induces the phosphorylation of SOS1 at Ser1164 and Ser1196. However, a functional significance of this phosphorylation event could not be confirmed.

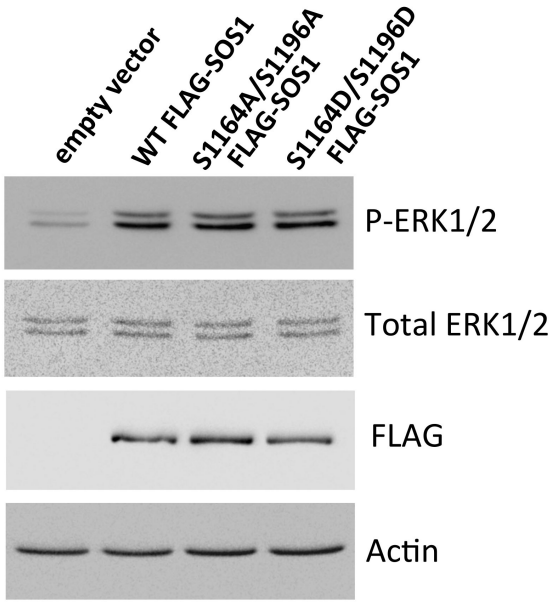

Figure 23. Effect of overexpression of wild type and mutant SOS1 on ERK1/2 phosphorylation. HEK 293T cells were transfected with the indicated expression plasmids. Two days after transfection, cells were lysed and cell lysates were analysed by Western blotting with the indicated antibodies.

4. DISCUSSION

Cif has previously been shown to inhibit CRL function (Cui *et al.*, 2010). CRL inhibition is due to a novel mechanism that involves a unique deamidation of Nedd8, which is a ubiquitin-like protein that is conjugated to cullin proteins and necessary for CRL activation. Here I provide evidence for a novel function of Cif that is independent of CRL inhibition but dependent on its deamidase activity. I found that Cif expression induces marked ERK phosphorylation and thus leads to the activation of ERK MAPK signaling, indicating that Cif has an effect on cellular signaling. Importantly, my results suggest that Cif deamidase likely has other downstream targets in addition to Nedd8.

My results suggest that Cif acts at the level of SOS1 via a novel mechanism that potentially involves SOS1 phosphorylation. Thus, Cif caused slower mobility of SOS1 and SOS1 deletion analysis suggested that this effect is mediated via a region in SOS1 that comprises the CDC25-H and proline-rich domains. Protein deamidation has been found to cause an increase in protein mobility in native gels, but is without effect on protein migration in SDS gels (Cui *et al.*, 2010). Hence, the observed SOS1 mobility change upon Cif co-expression is most likely due to one or more phosphorylation events. To confirm this, I used phosphatase treatment of lysates from SOS1 and Cif expressing cells. However surprisingly, treatment with calf intestine alkaline phosphatase or shrimp alkaline phosphatase was unable to reverse the slower migration of SOS1. A positive control experiment indicated that FRAT1 could be dephosphorylated under the same conditions. This suggests that the

observed mobility change in SOS1 is due to a protein modification different from phosphorylation or deamidation. Alternatively, it is possible that the Cif-induced phosphorylation site(s) in SOS1 are resistant to alkaline phosphatase treatment.

To distinguish between the different possibilities that might be responsible for the SOS1 mobility change, we analysed SOS1 post-translational modifications by mass spectrometry. Full length SOS1 was isolated from cell lysates after expression of FLAG-mSOS1 in the absence or presence of Cif. Three repeat experiments were performed and detailed analysis of the detected tryptic peptides showed a great number of deamidation and phosphorylation sites in the mouse SOS1 protein. However, only two sites, Ser1164 and Ser1196, showed a consistent Cif-dependent increase in phosphorylation. Importantly, based on the mSOS1 deletion construct experiments, these two residues are located in the region of Cif that is responsible for the Cif-induced mobility change. Of note, the corresponding two serine residues in human SOS1 have been previously identified in a large-scale phosphoproteomics study to be phosphorylated (Zhou *et al.*, 2013). However, so far there are no reports on the functional role of these phosphorylation events.

I then proceeded to confirm the Cif-dependent phosphorylation of Ser1164 and Ser1196 and characterise the functional significance by performing mutagenesis experiments. The S1164A/S1196A SOS1 mutant was at least partially resistant to Cif-induced phosphorylation. This indicated that the Cif-induced mobility change in SOS1 is indeed caused by

phosphorylation events and that these are at least partially accounted for by the phosphorylation of Ser1164 and Ser1196.

It is very intriguing that the two phosphorylation sites are located at equivalent sites immediately upstream of two PxxPxR motifs in SOS1. Although these motifs are known to be involved in binding of SOS1 to the SH3 domain of Grb2, I did not observe an effect of Cif expression on the interaction between SOS1 and Grb2. However, it would be interesting to determine whether the Ser1164 and Ser1196 SOS1 mutants generated in my study display altered binding to Grb2.

I conducted further experiments using the mutants to determine whether the Cif-induced phosphorylation of SOS1 is functionally important for the regulation of MAPK/ERK signaling. I found that overexpressing the non-phosphorylatable SOS1 S1164A/S1196A mutant did not prevent Cif-induced MAPK/ERK activation. However, this does not rule out that Cif-induced Ser1164 and Ser1196 phosphorylation is functionally significant as endogenous SOS1 was still expressed. In future work, it would hence be important to simultaneously transfect cells with siRNA targeting endogenous SOS1 and siRNA-resistant wild type and S1164A/S1196A mutant SOS1 expression plasmids. This experiment would be expected to be more conclusive in determining the role of Cif-induced SOS1 phosphorylation in ERK activation.

I also found that overexpression of the S1164D/S1196D mutant of SOS1 did not mimic MAPK/ERK activation induced by Cif. Mutation of serine or threonine residues to aspartate often mimics phosphorylation and elicits

similar downstream effects. However, it is important to note that this is not the case in every instance. Hence, a lack of effect of phosphomimetic mutants does not rule out a functional significance of a phosphorylation event. Taken together, although the experiments presented did not provide support for a role of Ser1164 and Ser1196 phosphorylation in Cif-induced MAPK/ERK activation, the results do not disprove such a role and further studies will be required. However, it is also possible that Cif induces the phosphorylation of other residues in SOS1 that were not detected in our proteomics study or activates MAP/ERK by inducing other post-translational modifications.

The mechanism through which Cif alters SOS1 function is currently not clear. My experiments suggest that Cif causes modification of SOS1 in a region that comprises the CDC25-H and proline-rich domains. The CDC25-H domain, together with the REM domain, mediates Ras nucleotide exchange. The C-terminal region has been suggested to exert a negative regulatory effect on the activity of human SOS1 (Corbalan-Garcia *et al*., 1998; Kim *et al*., 1998; Hall *et al*., 2002). Therefore, it is possible that by modifying these domains, Cif regulates SOS1 catalytic activity or alternatively downregulates or reverses the negative regulatory effects of the C-terminal region of SOS1. This would enhance the GEF activity of SOS1 and hence promote Ras activation and downstream signaling events. However, it is also possible that Cif functions to activate Ras via a different mechanism.

Importantly, my results raise the interesting possibility of the existence of an upstream regulator of SOS1 that can lead to a marked activation of ERK signaling. So far, SOS1 phosphorylation by different protein kinases has been

found to mainly play a negative regulatory role on ERK MAPK signaling (Kamioka *et al*., 2010). Thus, identification of the mechanism underlying Cif-dependent ERK MAPK activation is likely to provide novel insights into the regulation of this important signaling pathway.

How Cif promotes the pathogenicity of *B. pseudomallei* is currently not well characterised. It was originally proposed that Cif promotes the intracellular bacterial replication by inhibiting the turnover of epithelial host cells (Kim *et al*., 2010). This effect is due to cell cycle arrest as a result of the Cif-mediated inhibition of CRL-mediated degradation of cell cycle inhibitors such as p27. However, in a recent paper by McCormack *et al*. (2015), it was demonstrated that during *Yersinia pseudotuberculosis* infection, Cif plays a role to inhibit the activity of perforin-2, a mediator of the innate immune response of host cells. The authors found that upon *Y. pseudotuberculosis* infection, perforin-2 becomes activated through monoubiquitination. Perforin-2 ubiquitination is mediated via the CRL $SCF^{\beta\text{-TrCP}}$ and this results in the translocation of perforin-2 to cellular membranes, in particular the plasma and endosomal membranes. Upon translocation, perforin-2 then exerts its bactericidal activity by inducing lysis of plasma membrane-bound or endosome-encapsulated bacteria. Importantly, the authors demonstrated that *in vivo* Cif increases *Y. pseudotuberculosis* virulence in wild type but not perforin-2 deficient mice. This indicates that inhibiting the perforin-2 dependent host response is the primary function of Cif in *Y. pseudotuberculosis*.

However, the described mechanism in *Y. pseudotuberculosis* infection is unlikely to be of major relevance during the infection with Cif-expressing *B. pseudomallei*. This is because *B. pseudomallei* can readily escape from the endosomes into the host cytosol (Stevens *et al*., 2002; Muangsombut *et al*., 2008; Burtnick *et al*., 2008), thus avoiding the bactericidal activity of perforin-2. As such, it is likely that perforin-2 does not play a major role in the response of host cells to *B. pseudomallei* infection. My study suggests an alternative mechanism through which Cif may potentially exert its cellular effect. Prolonged CRL inhibition is known to induce cellular apoptosis. This is partly due to prevention of the degradation of key cell cycle regulatory proteins, including the important DNA replication licensing factor CDT1. Failure to degrade CDT1 leads to DNA re-replication and induction of cellular apoptosis (Milhollen *et al*., 2011). Given that host cell apoptosis would also limit bacterial replication and survival, I hypothesised that Cif may counteract the pro-apoptotic effects of CRL inhibition by activating cellular anti-apoptotic pathways through ERK activation. I indeed observed that Cif expression increased the phosphorylation of the most abundant Bim splice variant Bim_{EL} in an ERK1/2-dependent manner. ERK1/2-dependent phosphorylation is well known to induce proteasome-dependent Bim_{EL} protein degradation. Surprisingly, despite inducing marked Bim_{EL} phosphorylation, Cif reduced the Bim_{EL} steady state protein levels only slightly. It may be necessary to carry out half-life measurements of endogenous Bim_{EL} protein to detect Cif-induced changes in Bim_{EL} protein stability. I also observed that Cif increased the expression of the anti-apoptotic protein Mcl-1 and the phosphorylation of Bad,

leading to inhibition of its pro-apoptotic function (see Figure 4C). However, these effects were largely ERK independent as they were not or only slightly inhibited in the presence of MEK inhibitor. Interestingly, I also observed that expression of Cif could protect HEK293T cells from serum starvation-induced cell death (data not shown), suggesting that Cif-induced anti-apoptotic responses via the MAPK/ERK pathway are important. Hence, it would be of great interest to test whether Cif-dependent ERK MAPK activation and the induction of anti-apoptotic pathways is important to prevent host cell apoptosis and promote *B. pseudomallei* virulence *in vivo*.

In conclusion, I have identified a novel deamidation-dependent mechanism of action of the *B. pseudomallei* virulence factor Cif to activate MAPK/ERK signaling. The elucidation of the exact molecular mechanism is expected to give important new insights into the regulation of the MAPK/ERK signaling pathway. My study demonstrates that bacterial proteins such as Cif can serve as useful molecular tools to uncover novel aspects of mammalian signaling pathways.

REFERENCES

Asche, V. 1991. Melioidosis – a disease for all organs. *Today's Life Sci* June: 34–40.

Bartelt, R.R, Light, J., Vacaflores, A., Butcher, A., Pandian, M., Nash, P., Houtman, J.C. 2015. Regions outside of conserved PxxPxR motifs drive the high affinity interaction of GRB2 with SH3 domain ligands. *Biochim Biophys Acta.* Oct;1853(10 Pt A):2560-9.

Boh, B.K., Ng, M.Y., Leck, Y.C., Shaw, B., Long, J., Sun, G.W., Gan, Y.H. et al. 2011. Inhibition of Cullin RING ligases by Cycle Inhibiting Factor: evidence for interference with Nedd8-induced conformational control. *J. Mol. Biol*. 413, 430-437.

Bosu, D.R. and Kipreos, E.T. 2008. Cullin-RING ubiquitin ligases: global regulation and activation cycles. *Cell Div*. 3: 7.

Burtnick, M.N., Brett, P.J., Nair, V., Warawa, J.M., Woods, D.E., and Gherardini, F.C. 2008. *Burkholderia pseudomallei* type III secretion system mutants exhibit delayed vacuolar escape phenotypes in RAW 264.7 murine macrophages. *Infect. Immun*. 76, 2991–3000.

Carrano, A.C., Eytan, E., Hershko, A., Pagano, M. 1999. SKP2 is required for ubiquitin-mediated degradation of the CDK inhibitor p27. *Nat Cell Biol*. 1: 193–199.

Chaowagul, W. 2000. Recent advances in the treatment of severe melioidosis. *Acta Tropica* 74: 133–137.

Cheng, A.C. and Currie, B.J. 2005. Melioidosis: epidemiology, pathophysiology, and management. *Clin. Microbiol. Rev*. 18:383–416.

Chew, E.H., Poobalasingam, T., Hawkey, C.J., Hagen, T. 2007. Characterization of cullin-based E3 ubiquitin ligases in intact mammalian cells--evidence for cullin dimerization. *Cell Signal*. 19: 1071-1080.

Corbalan-Garcia, S., Margarit, S.M., Galron, D., Yang, S.S., Bar-Sagi, D. 1998. Regulation of Sos activity by intramolecular interactions. *Mol Cell Biol.* 18: 880-886.

Cornelis, G.R. 2006. The type II secretion injectisome. *Nature Rev. Microbiol.* 4, 811-825.

Cui, J., Yao, Q., Li, S., Ding, X., Lu, Q., Mao, H. et al. 2010. Glutamine deamidation and dysfunction of ubiquitin/NEDD8 induced by a bacterial effector family. *Science*, 329, 1215–1218.

Currie, B.J., Fisher, D.A., Howard, D.M., Burrow, J.N.C., Selvanayagam, S., Snelling, P.L., Anstey, N.M., Mayo, M.J. 2000. The epidemiology of melioidosis in Australia and Papua New Guinea. *Acta Tropica* 74: 121–127.

Dance, D.A.B. 1991. Melioidosis: the tips of the iceberg? *Clin Microbiol Rev* 4: 52–60.

De Rycke, J., Comtet, E., Chalareng, C., Boury, M., Tasca, C., Milon, A. (1997). Enteropathogenic *Escherichia coli* O103 from rabbit elicits actin stress fibers and focal adhesions in HeLa epithelial cells, cytopathic effects that are linked to an analog of the locus of enterocyte effacement. *Infect Immun* 65: 2555-2563.

Dharakul, T. and Songsivilai, S. 1999. The many facets of melioidosis. *Trends Microbiol.* 7: 138–140.

Douville, E. and Downward, J. 1997. EGF induced SOS phosphorylation in PC12 cells involves P90 RSK-2. *Oncogene.* 15: 373-383.

Gan, Y.H., Chua, K.L., Chua, H.H., Liu, B., Hii, C.S., Chong, H.L., and Tan, P. 2002. Characterization of *Burkholderia pseudomallei* infection and identification of novel virulence factors using a *Caenorhabditis elegans* host system. *Mol. Microbiol*. 44, 1185–1197.

Galyov, E.E., Brett, P.J., DeShazer, D. 2010. Molecular insights into *Burkholderia pseudomallei* and *Burkholderia mallei* pathogenesis. *Annu Rev Microbiol* 64:495–517.

Groves, J.T. and Kuriyan, J. 2010. Molecular mechanisms in signal transduction at the membrane. *Nat Struct Mol Biol*. 17: 659-665.

Gupta, R.W. and Mayer, B.J. 1998. Dominant-negative mutants of the SH2/SH3 adapters Nck and Grb2 inhibit MAP kinase activation and mesoderm-specific gene induction by eFGF in Xenopus. *Oncogene*. 17: 2155-2165.

Hall, B.E., Yang, S.S., Bar-Sagi, D. 2002. Autoinhibition of Sos by intramolecular interactions. *Front Biosci*. 1: d288-d294.

Holden, M.T., Titball, R.W., Peacock, S.J., Cerden o-Ta rraga, A.M., Atkins, T., Crossman, L.C., Pitt, T., Churcher, C., Mungall, K., Bentley, S.D., et al. 2004. Genomic plasticity of the causative agent of melioidosis, *Burkholderia pseudomallei*. *Proc. Natl. Acad. Sci*. USA 101, 14240–14245.

Inglis, T.J., Rigby, P., Robertson, T.A., Dutton, N.S., Henderson, M., and Chang, B.J. 2000. Interaction between *Burkholderia pseudomallei* and *Acanthamoeba* species results in coiling phagocytosis, endamebic bacterial survival, and escape. *Infect. Immun.* 68, 1681–1686.

Jani, A.J. and Cotter, P.A. 2010. Type VI secretion: not just for pathogenesis anymore. *Cell Host Microbe* **8**, 2–6.

Jones, A.L., Beveridge, T.J., Woods, D.E. 1996. Intracellular survival of *Burkholderia pseudomallei*. *Infect Immun* 64(3):782–790.

Jubelin, G., Chavez, C.V., Taieb, F., Banfield, M.J., Samna-Louaka, A., Nobe, R., Nougayrede, J.P., Zumbihl, R., Givaudan, A., Escoubas, J.M., Oswald, E. 2009. Cycle inhibiting factors (CIFs) are a growing family of functional cyclomodulins present in invertebrate and mammal bacterial pathogens. *PLoS ONE* **4**(3):e4855.

Jubelin, G., Taieb, F., Duda, D.M., Hsu, Y., Samba-Louaka, A., Nobe, R., Penary, M., Watrin, C., Nougayrède, J.P., Schulman, B.A., Stebbins, C.E., Oswald, E. 2010. Pathogenic bacteria target NEDD8-conjugated cullins to hijack host-cell signaling pathways. *PLoS Pathog*. 2010:6: e1001128.

Kamioka, Y., Yasuda, S., Fujita, Y., Aoki, K., Matsuda, M. 2010. Multiple decisive phosphorylation sites for the negative feedback regulation of SOS1 via ERK. *J Biol Chem*. 285: 33540-33548.

Kim, J.H., Shirouzu, M., Kataoka, T., Bowtell, D., Yokoyama, S. 1998. Activation of Ras and its downstream extracellular signal-regulated protein kinases by the CDC25 homology domain of mouse Son-of-sevenless 1 (mSos1). *Oncogene*. 16: 2597-2607.

Kim, M., Ashida, H., Ogawa, M., Yoshikawa, Y., Mimuro, H., Sasakawa, C. 2010. Bacterial interactions with the host epithelium. *Cell Host Microbe* **8**, 20-35.

Lee, Y.H., Chen, Y., Ouyang, X., and Gan, Y.H. (2010). Identification of tomato plant as a novel host model for *Burkholderia pseudomallei*. *BMC Microbiol.* 10, 28.

Leelarasamee, A. 2000. Melioidosis in southeast Asia. *Acta Tropica* 74: 129–132.

Ley, R., Ewings, K.E., Hadfield, K., Cook, S.J. 2005. Regulatory phosphorylatiog of Bim: sorting out the ERK from the JNK. *Cell Death Differ*. 12:1008-1014.

McCormack, R.M., Lyapichev, K., Olsson, M.L., Podack, E.R., Munson, G.P. 2015. Enteric pathogens deploy cell cycle inhibiting factors to block the bactericidal activity of Perforin-2. *eLife*. 2015;4: e06505.

Milhollen, M.A., Narayanan, U., Soucy, T.A., Veiby, P.O., Smith, P.G., Amidon, B. 2011. Inhibition of Nedd8-activating enzyme induces rereplication and apoptosis in human tumor cells consistent with deregulating CDT1

turnover. *Cancer Res.* 71: 3042-3051.

Morikawa, H., Kim, M., Mimuro, H., Punginelli, C., Koyama, T., Nagai, S.. Miyawaki, A., Iwai, K., Sasakawa, C. 2010. The bacterial effector Cif interferes with SCF ubiquitin ligase function by inhibiting deneddylation of Cullin1. *Biochem Biophys Res Commun*. 2010:401: 268–274.

Mota, L.J. and Cornelis, G.R. 2005. The bacterial injection kit: type III secretion systems. *Ann. Med*. **37**, 234-249.
Muangsombut, V., Suparak, S., Pumirat, P., Damnin, S., Vattanaviboon, P., Thongboonkerd, V, *et al*. 2008. Inactivation of *Burkholderia pseudomallei* bsaQ results in decreased invasion efficiency and delayed escape of bacteria from endocytic vesicles. *Arch Microbiol*. 190: 623-631.

Nassar N, Singh K, Garcia-Diaz M. 2010. Structure of the dominant negative S17N mutant of Ras. *Biochemistry*. 49: 1970-1974.

Ngauy, V., Lemeshev, Y., Sadkowski, L., Crawford, G. 2005. Cutaneous melioidosis in a man who was taken as a prisoner of war by the Japanese duringWorld War II. J. *Clin. Microbiol*. 43:970–72.

Petroski, M.D. and Deshaies, R.J. 2005. Function and regulation of cullin-RING ubiquitin ligases. *Nat Rev Mol Cell Biol*. 6: 19–20.

Rojas, J.M., Oliva, J.L., Santos, E. 2011. Mammalian Son of Sevenless guanine nucleotide exchange factors: old concepts and new perspectives. *Genes Cancer*. 2: 298-305.

Samba-Louaka, A., Nougayrde, J.P., Watrin, C., Jubelin, G., Oswald, E., Taieb, F. 2008. Bacterial cyclomodulin Cif blocks the host cell cycle by stabilizing the cyclin-dependent kinase inhibitors p21 and p27. *Cell Microbiol*. 10: 2496–2508.

Soucy, T.A., Smith, P.G., Milhollen, M.A., Berger, A.J., Gavin, J.M. et al. 2009. An inhibitor of Nedd8-activating enzyme as a new approach to treat cancer. *Nature*. **458**, 732-736.

Sprague, L.D., and Neubauer, H. 2004. Melioidosis in animals: a review on epizootiology, diagnosis and clinical presentation. *J. Vet. Med. B Infect. Dis. Vet. Public Health* 51, 305–320.

Stevens, M.P., Wood, M.W., Taylor, L.A., Monaghan, P., Hawes, P., Jones, P.W., Wallis, T.S., and Galyov, E.E. 2002. An Inv/Mxi-Spa-like type III protein secretion system in *Burkholderia pseudomallei* modulates intracellular behavior of the pathogen. *Mol. Microbiol*. 46, 649–659.

Stevens, M.P., Haque, A., Atkins, T., Hill, J., Wood, M.W., Easton, A., Nelson, M., Underwood-Fowler, C., Titball, R.W., Bancroft, G.J., Galyov, E.E. 2004. Attenuated virulence and protective efficacy of a *Burkholderia pseudomallei* bsa type III secretion mutant in murine models of melioidosis. *Microbiology* 150(Pt 8):2669–2676.

Suputtamongkol, Y., Hall, A.J., Dance, D.A.B., Chaowagul, W., Wajchanuvong, A., Smith, M.D., and White, N.J. 1994. The epidemiology of melioidosis in Ubon Ratchatani, northeast Thailand. *Int J Epidemiol* 23: 1082–1090.

Sutterlüty, H., Chatelain, E., Marti, A., Wirbelauer, C., Senften, M., Müller, U., Krek, W. 1999. p45SKP2 promotes p27Kip1 degradation and induces S phase in quiescent cells. *Nat Cell Biol*. 1: 207–214.

Taieb, F., Nougayrède, J.P., Oswald, E. 2011. Cycle Inhibiting Factors (Cifs): cyclomodulins that usurp the ubiquitin-dependent degradation pathway of host cells. *Toxins (Basel)*. 3: 356-368.

Tanaka, M., Gupta, R.W., Mayer, B.J. 1995. Differential inhibition of signaling pathways by dominant-negative SH2/SH3 adapter proteins. *Mol Cell Biol.* 15: 6829-6837.

Tsvetkov, L.M., Yeh, K.H., Lee, S.J., Sun, H., Zhang, H. 1999. p27(Kip1) ubiquitination and degradation is regulated by the SCF(Skp2) complex through phosphorylated Thr187 in p27. *Curr Biol.* 9: 661–664.

Yao, Q., Cui, J., Zhu, Y., Wang, G., Hu, L., Long, C., Cao, R., Liu, X., Huang, N., Chen, S., Liu, L., Shao, F. 2009. A bacterial type III effector family uses the papain-like hydrolytic activity to arrest the host cell cycle. *PNAS* **106**(10), 3716-3721.

Yasuda, R., Harvey, C.D., Zhong, H., Sobczyk, A., van Aelst, L., Svoboda, K. 2006. Supersensitive Ras activation in dendrites and spines revealed by two-photon fluorescence lifetime imaging. *Nat Neurosci*. 9: 283-291.

Yu, C., Mao, H., Novitsky, E.J., Tang, X., Rychnovsky, S.D., Zheng, N., Huang, L. 2015. Gln40 deamidation blocks structural reconfiguration and activation of SCF ubiquitin ligase complex by Nedd8. *Nat. Commun*. 6: 10053.

Warawa, J., Woods, D.E. 2005. Type III secretion system cluster 3 is required for maximal virulence of *Burkholderia pseudomallei* in a hamster infection model. *FEMS Microbiol Lett* 242(1):101–108.

White, N.J. 2003. Melioidosis. *Lancet* 361:1715–22.

Wiersinga, W.J., van der Poll, T., White, N.J., Day, N.P., Peacock, S.J. 2006. Melioidosis: insights into the pathogenicity of *Burkholderia pseudomallei*. *Nat Rev Microbiol* 4(4):272–282.

Zhou, H., Di Palma, S., Preisinger, C., Peng, M., Polat, A.N., Heck, A.J., Mohammed, S. 2013. Toward a comprehensive characterization of a human cancer cell phosphoproteome. *J Proteome Res.* Jan 4;12(1):260-71.